Technical University of Crete
School of Production Engineering and Management

Real-Time Control of Smart Energy Buildings

DIPLOMA THESIS

Eleftherios G. Kyriakou

EXAMINING COMMITTEE

Associate Professor Ipsakis Dimitrios (Supervisor)

Professor Kouikoglou Vassilis

Associate Professor Kanellos Fotios (School of ECE, TUC)

Chania, Crete, July 2024

Πολυτεχνείο Κρήτης
Σχολή Μηχανικών Παραγωγής και Διοίκησης

Έλεγχος σε πραγματικό χρόνο για έξυπνα ενεργειακά κτίρια

ΔΙΠΛΩΜΑΤΙΚΗ ΕΡΓΑΣΙΑ

Ελευθέριος Γ. Κυριάκου

ΕΞΕΤΑΣΤΙΚΗ ΕΠΙΤΡΟΠΗ

Αναπληρωτής Καθηγητής Ιψάκης Δημήτριος (Επιβλέπων)

Καθηγητής Κουϊκόγλου Βασίλειος

Αναπληρωτής Καθηγητής Κανέλλος Φώτιος (Σχολή ΗΜΜΥ, Πολυτεχνείο Κρήτης)

Χανιά, Κρήτη, Ιούλιος 2024

Acknowledgements

First and foremost, I would like to express my sincere thanks to my supervisor, Professor Ipsakis Dimitrios, for his valuable assistance and continuous support, throughout my diploma thesis. I am sincerely grateful to Professor Kanellos Fotios for his guidance and his extensive research experience, activity, and knowledge that have inspired me.

I would also like to thank my committee member Kouikoglou Vassilis for his helpful comments and time.

Last, but not least, I would like to express my deepest gratitude to my family and close friends for their love, support, encouragement, and trust.

Chania, July 2024
Eleftherios G. Kyriakou

Abstract

The real-time management and control of Building Energy Systems (BES) is crucial for improving both energy resilience and efficiency. By utilizing real-time control alongside ongoing monitoring and adjusting to variations in energy supply and demand, BES ensures a consistent and dependable power supply for local areas, even during grid disruptions or power outages. Additionally, real-time operation facilitates demand response strategies, allowing users to effectively control their energy use and expenses. This approach is essential in updating and safeguarding modern energy infrastructure, contributing to its sustainability. In this work, system identification and parameter estimation techniques are used. The developed tools can be very useful in energy management and real-time control applications of building energy systems. A detailed model of the building energy system is also developed, which is the basis on which the applied identification techniques are based, as well as any real-time control system of the building energy system.

Περίληψη

Η λειτουργία των ενεργειακών συστημάτων κτιρίων σε πραγματικό χρόνο έχει ιδιαίτερη σημασία λόγω της ικανότητάς της να ενισχύει την ανθεκτικότητα και αποδοτικότητα ενεργειακών συστημάτων. Ο έλεγχος σε πραγματικό χρόνο, σε συνδυασμό με τη συνεχή παρακολούθηση και την προσαρμογή στις διακυμάνσεις της προσφοράς-ζήτησης ενέργειας, εξασφαλίζει σταθερή και αξιόπιστη παροχή ενέργειας στις τοπικές κοινότητες, ακόμη και κατά τη διάρκεια διαταραχών ή διακοπών του δικτύου. Επιπλέον, η λειτουργία σε πραγματικό χρόνο υποστηρίζει μηχανισμούς απόκρισης στη ζήτηση, επιτρέποντας στους χρήστες να διαχειρίζονται ενεργά την κατανάλωση ενέργειας και το κόστος της. Συνολικά, διαδραματίζει καθοριστικό ρόλο στον εκσυγχρονισμό και τη μελλοντική διασφάλιση της σύγχρονης ενεργειακής υποδομής, καθιστώντας την πιο βιώσιμη.

Στην παρούσα εργασία γίνεται χρήση τεχνικών αναγνώρισης συστήματος και εκτίμησης παραμέτρων. Τα αναπτυχθέντα εργαλεία μπορούν να είναι πολύ χρήσιμα σε εφαρμογές διαχείρισης ενέργειας και ελέγχου πραγματικού χρόνου κτιριακών ενεργειακών συστημάτων. Επίσης, αναπτύσσεται λεπτομερές μοντέλο του κτιριακού ενεργειακού συστήματος, το οποίο αποτελεί τη βάση που στηρίζονται οι εφαρμοσθείσες τεχνικές αναγνώρισης, καθώς και όποιο σύστημα ελέγχου πραγματικού χρόνου του ενεργειακού συστήματος του κτιρίου.

Η χρήση της ομαδοποίησης K-means σε δεδομένα εσωτερικής θερμοκρασίας θερμικών ζωνών κτιρίων αποσκοπεί στην ταξινόμηση αυτών των ζωνών σε ομάδες με παρόμοια μοτίβα θερμοκρασίας. Ο πρωταρχικός στόχος είναι ο εντοπισμός και η ομαδοποίηση παρόμοιων μοτίβων θερμοκρασίας εντός των θερμικών ζωνών του κτιρίου. Κάθε συστάδα αντιπροσωπεύει ένα σύνολο θερμικών ζωνών που παρουσιάζουν παρόμοια συμπεριφορά θερμοκρασίας. Με την ομαδοποίηση των δεδομένων θερμοκρασίας, μπορούμε να χαρακτηρίσουμε διαφορετικούς τύπους θερμικών ζωνών εντός του κτιρίου. Για παράδειγμα, ορισμένες συστάδες μπορεί να αντιστοιχούν σε δωμάτια που είναι γενικά θερμότερα, ψυχρότερα ή έχουν πιο σταθερές θερμοκρασίες. Η κατανόηση αυτών των συστάδων μπορεί να βοηθήσει στη βελτιστοποίηση των συστημάτων θέρμανσης, εξαερισμού και κλιματισμού. Με την αναγνώριση ζωνών με παρόμοια προφίλ θερμοκρασίας, το σύστημα θέρμανσης - ψύξης μπορεί να διαχειριστεί πιο αποτελεσματικά για τη διατήρηση των επιθυμητών θερμοκρασιών, οδηγώντας ενδεχομένως σε εξοικονόμηση ενέργειας.

Συγκεκριμένα, στο πρώτο μέρος της εργασίας, αναπτύχθηκε ένα ακριβές μοντέλο για την εκτίμηση της εσωτερικής θερμοκρασίας των θερμικών ζωνών του κτιρίου, το οποίο είναι ζωτικής σημασίας για τη διαχείριση της ενέργειας και την άνεση των ενοίκων. Το μοντέλο χρησιμοποιεί τέσσερις βασικές εισόδους: τα εσωτερικά θερμικά φορτία εντός των θερμικών ζωνών, τα οποία περιλαμβάνουν τη θερμότητα που παράγεται από τους ανθρώπους, τον

φωτισμό και τις ηλεκτρικές και ηλεκτρονικές συσκευές, την κατανάλωση ενέργειας του συστήματος θέρμανσης - ψύξης, τη θερμοκρασία περιβάλλοντος, η οποία επηρεάζει τη θερμική ισορροπία μεταξύ του κτιρίου και του περιβάλλοντός του, και την ηλιακή ακτινοβολία, η οποία επηρεάζει τη θερμοκρασία του εσωτερικού χώρου μέσω της άμεσης και έμμεσης θέρμανσης. Για να το πετύχουμε αυτό, εφαρμόζουμε προηγμένες τεχνικές μοντελοποίησης, συγκεκριμένα την αναγνώριση συστημάτων και τα νευρωνικά δίκτυα. Η αναγνώριση συστήματος περιλαμβάνει τη δημιουργία μαθηματικών μοντέλων με βάση τα παρατηρούμενα δεδομένα για την αποτύπωση της δυναμικής συμπεριφοράς των θερμικών ζωνών, ενώ τα νευρωνικά δίκτυα προσφέρουν μια προσέγγιση με βάση τα δεδομένα για την εκμάθηση πολύπλοκων, μη γραμμικών σχέσεων μεταξύ των εισόδων και της εσωτερικής θερμοκρασίας.

Στο δεύτερο μέρος της εργασίας, γίνεται χρήση τεχνικών εκτίμησης παραμέτρων. Οι τεχνικές εκτίμησης παραμέτρων είναι συμβάλουν σημαντικά στην αποδοτικότητα, την αξιοπιστία και τη βελτιστοποίηση της χρήσης ενέργειας. Η ακριβής εκτίμηση παραμέτρων αποτελεί τη βάση για αξιόπιστα ενεργειακά μοντέλα, ενισχύοντας την ακρίβεια πρόβλεψης και επιτρέποντας καλύτερο σχεδιασμό και κατανομή πόρων.

Συγκεκριμένα, η εργασία αυτή παρουσιάζει μια εξελιγμένη προσέγγιση για τη διαχείριση της ενέργειας του κτιρίου σε πραγματικό χρόνο μέσω της ακριβούς εκτίμησης των εσωτερικών θερμικών κερδών. Αξιοποιώντας ένα θερμικό μοντέλο κτιρίου και χρησιμοποιώντας τον αλγόριθμο βελτιστοποίηση σμήνους σωματιδίων, ελαχιστοποιούνται οι αποκλίσεις μεταξύ των εκτιμώμενων και των πραγματικών εσωτερικών θερμοκρασιών των θερμικών ζωνών του κτιρίου, οδηγώντας σε βελτιστοποιημένη απόδοση των συστημάτων θέρμανσης - ψύξης και βελτιώνοντας τις συνθήκες άνεσης των ενοίκων. Πιο αναλυτικά, το θερμικό μοντέλο του κτιρίου εκτιμά την εσωτερική θερμοκρασία για κάθε θερμική ζώνη χρησιμοποιώντας τις δεδομένες εισόδους. Οι εκτιμώμενες εσωτερικές θερμοκρασίες συγκρίνονται με τις πραγματικές εσωτερικές θερμοκρασίες που έχουν μετρηθεί στο κτίριο. Το σφάλμα για κάθε θερμική ζώνη υπολογίζεται ως η διαφορά μεταξύ της εκτιμώμενης και της πραγματικής εσωτερικής θερμοκρασίας. Τα σφάλματα από όλες τις θερμικές ζώνες αθροίζονται για να σχηματιστεί η αντικειμενική συνάρτηση. Ο αλγόριθμος PSO ρυθμίζει επαναληπτικά τα εκτιμώμενα εσωτερικά θερμικά κέρδη για την ελαχιστοποίηση της αντικειμενικής συνάρτησης, μειώνοντας έτσι το συνολικό σφάλμα και ευθυγραμμίζοντας τις εκτιμώμενες εσωτερικές θερμοκρασίες με τις πραγματικές μετρήσεις. Η μεθοδολογία καταδεικνύει την αποτελεσματικότητα της χρήσης δεδομένων εισόδου σε πραγματικό χρόνο, όπως η θερμοκρασία περιβάλλοντος, η ηλιακή ακτινοβολία και η κατανάλωση ισχύος των συστημάτων θέρμανσης - ψύξης, για τη βελτίωση των προβλέψεων του μοντέλου και τη διασφάλιση ενεργειακά αποδοτικών λειτουργιών του κτιρίου. Η ενσωμάτωση του τυχαιοκρατικού αλγορίθμου βελτιστοποίησης σμήνους σωματιδίων σε αυτό το πλαίσιο υπογραμμίζει τις δυνατότητές του

στην επίλυση σύνθετων προκλήσεων βελτιστοποίησης στο πλαίσιο της ενεργειακής διαχείρισης κτιρίων.

Contents

Nomenclature

Abbreviations

EMS Energy Management System
HVAC Heating, Ventilation and Air Conditioning
m.u. monetary unit

Sets and indices

$\mathcal{B}$, b buildings' set, building's number index
$\mathcal{E}$ external walls set
$\mathcal{I}$ internal walls set
$\mathcal{N}$ neighboring thermal zones set
x xth internal wall index
y yth external wall/window index
z zth thermal zone index

Parameters, constants and variables

β_z surface slop
θ, θ_z incidence angle, zenith angle
τ_{win} window glass transmission coefficient
a_{0g}, a_{1g}, a_{2g} gth generator FC coefficients
a_w the external wall absorbance coefficient
C_z specific heat capacity
COP coefficient of EC performance
EP Variable price of electricity (m.u./kWh)
F_{wall}, F_{win} wall/window surface area
$FL_z^{\uparrow}$ flexibility of a thermal zone to increase its power demand
$FL_z^{\downarrow}$ flexibility of a thermal zone to decrease its power demand
I_b, I_d, I beam, diffuse and total radiation on horizontal surface, respectively
$I_{T,z}$ total solar radiation
N_z thermal zones total number
ρ density of thermal zone
$P_{HVAC,b}$ Building's electric power consumption for cooling (kW)
$P_{HVAC,b,max}$,$P_{HVAC,b,min}$ Building's HVAC power consumption boundaries (kW)
$P_{HVAC,z}$ Thermal zone's electric power consumption for cooling (kW)
$P_{HVAC,z,max}$,$P_{HVAC,z,min}$ Thermal zone's HVAC power consumption boundaries (kW)
$Q_{HVAC,z}$ thermal zone's power production for cooling (kW)
$\dot{Q}_{ex,wall,z}$ external walls heat exchange (kW)
$\dot{Q}_{in,wall,z}$ internal walls heat exchange (kW)
$Q_{in,z}$ internal heat gains f (kW)
$\dot{Q}_{sg,z}$ solar radiation through the windows (kW)
$\dot{Q}_{sw,z}$ heat gain of external walls' solar radiation (kW)
$\dot{Q}_{win,z}$ heat transfer across the windows (kW)
R_{se} heat resistance of the external surface
SC the shading coefficient of the windows
$T_{in,nz}$ indoor temperature of the neighbor thermal zone

$T_{in,z}$ thermal zone's temperature (°C)

$T_{max,z}, T_{min,z}$ thermal zone's temperature boundaries (°C)

T_{out} outdoor temperature (°C)

SC the shading coefficient of the windows

U_{wall}, U_{win} factor of the heat exchange of the external wall/window

V_z volume of the air of the zth thermal zone

Chapter 1

Introduction

1.1. General

As urbanization accelerates and energy demand increases, buildings continue to be a key contributor to overall energy consumption. Energy consumption in the building sector is a key issue both at national and European Union (EU) level. In Greece, buildings contribute 65% of electricity demand, with this figure reaching 85% for the non-interconnected islands, in particular as a result of consumption due to the tourism sector. It is expected that any energy-efficient building policies could lead to a 5-6% reduction in overall energy consumption at EU level and a corresponding 5% reduction in CO2 emissions [1]. The International Energy Agency estimates that a high efficiency building envelope can lead to a significant reduction in the energy demand of a typical building, which can reach 20-30% in cold climates and 10-40% in hot climates. [2].

In general, heating and cooling loads, along with the energy needed for the production of hot water, contribute almost 60% of the total energy consumption of buildings. Therefore, the need for innovative technologies for smart building energy management systems at different levels of integration is more urgent than ever. Through the application of sophisticated real-time control techniques, HVAC systems can be dynamically adapted to align with real-time conditions, usage patterns, and energy availability. R**eal-time control allows buildings to seamlessly integrate with smart grids, take part in demand response initiatives, and enhance the quality of life by improving economics and ensuring comfort**.

1.2. Thesis Overview

Thesis is structured in the following sections. **Chapter 2** provides a brief state of the art related to building energy management and control. Building thermal loads mechanism modeling is included in **Chapter 3**. **Chapter 4** gives an overview of system identification, while the use of system identification in control of building energy systems and the respective results are provided in **Chapter 5**. Finally, **Chapter 6** presents parameter estimation in building energy management and control systems; while the respective conclusions and future extensions are drawn in **Chapter 7**.

Chapter 2

State of the Art

The importance of real-time building energy management and control lies in its ability to significantly enhance energy efficiency, reduce operational costs, and improve the comfort and well-being of occupants. By continuously monitoring and dynamically adjusting the performance of HVAC systems, lighting, and other energy-intensive operations, these systems can respond immediately to fluctuations in environmental conditions and occupancy levels. This real-time adaptability ensures optimal energy usage, prevents wastage, and maintains indoor environmental quality. Additionally, real-time control systems can integrate renewable energy sources and storage solutions more effectively, contributing to a building's sustainability goals. Participation in demand response programs allows buildings to adjust their energy consumption in response to grid demands, promoting grid stability and potentially earning financial incentives. The incorporation of advanced analytics and machine learning further enhances these systems, providing predictive insights and automated optimization that drive continuous improvement. Overall, real-time building energy management and control are crucial for advancing energy efficiency, sustainability, and economic viability in the built environment.

Energy management systems (EMS) for buildings frequently prioritize optimizing and controlling single buildings [3],[4] rather than focusing on managing microgrids comprising building complexes. Energy management strategies have predominantly concentrated on residential buildings [5],[6] and residential microgrids [7], which are simpler to optimize compared to the more complex and challenging commercial buildings and microgrids. A robust energy management method for microgrids operating in both grid-connected and autonomous mode is outlined in [8]-[10], unlike [11],[12], which do not consider the islanded operation of the microgrid. Specifically, [10] highlights that when the microgrid is connected to the main grid, the grid manages system frequency and voltage. During significant load variations in autonomous mode, a diesel generator takes over the regulation of frequency and voltage. Additionally, [13]-[15] propose an optimal energy management approach for controlling HVAC systems in commercial buildings. Furthermore, the EMS proposed in [16] classifies electrical loads into critical and non-critical categories and considers the building's thermal characteristics. This approach contrasts with [17], where different load types were not modeled independently.

Chapter 3

Building Thermal Loads Modeling

3.1 Modeling of Building Thermal Loads

In this thesis, each building is divided into thermal zones. The loads of the thermal zones of the building are calculated according to the technical specifications of the building, the occupancy, the level of activity, the different types of appliances used in each thermal zone, the conditioned space of each thermal zone, the outdoor temperature, solar radiation, etc. Using the following thermal equilibrium equation, the thermal behavior of a thermal zone is analyzed [18]-[24].

$$p \cdot C_z \cdot V_z \cdot \frac{dT_{in,z}}{dt} = \dot{Q}_{ex,wall,z} + \dot{Q}_{in,wall,z} + \dot{Q}_{win,z} + Q_{in,z} + \dot{Q}_{sw,z} + \dot{Q}_{sg,z} - Q_{HVAC,z} \quad (1)$$

The transfer of heat between a thermal zone and its surroundings is detailed by Equations (2)-(6).

$$\dot{Q}_{ex,wall,z} = \sum_{y \in \mathcal{E}} U_{wall,y} \cdot F_{wall,y} \cdot \left(T_{out} - T_{in,z}\right) \quad (2)$$

$$\dot{Q}_{win,z} = \sum_{y \in \mathcal{E}} U_{win,y} \cdot F_{win,y} \cdot \left(T_{out} - T_{in,z}\right) \quad (3)$$

$$\dot{Q}_{sw,z} = \sum_{y \in \mathcal{E}} a_w \cdot R_{se} \cdot U_{wall,y} \cdot F_{wall,y} \cdot I_{T,z} \quad (4)$$

$$\dot{Q}_{sg,z} = \sum_{y \in \mathcal{E}} \tau_{win} \cdot SC \cdot F_{win,y} \cdot I_{T,z} \quad (5)$$

$$\dot{Q}_{in,wall,z} = \sum_{y \in \mathcal{E}} U_{wall,y} \cdot F_{wall,y} \cdot \left(T_{in,nz} - T_{in,z}\right) \quad (6)$$

By appropriately modifying (1)-(6), the state space system of equations is obtained for each building.

$$\frac{d\boldsymbol{T_{in}}(t)}{dt} = \boldsymbol{A_b} \cdot \boldsymbol{T_{in}}(t) + \boldsymbol{B_b} \cdot \boldsymbol{U} \tag{7}$$

$$\boldsymbol{Y}(t) = \boldsymbol{C_b} \cdot \boldsymbol{T_{in}}(t) + \boldsymbol{D_b} \cdot \boldsymbol{U} \tag{8}$$

The input vector $\boldsymbol{U}$ is of dimension $(2N_Z + 2) \times 1$. It is given in (9).

$$\boldsymbol{U} = \begin{bmatrix} Q_{EC,1}(t) \\ \vdots \\ Q_{EC,N_Z}(t) \\ Q_{in,1}(t) \\ \vdots \\ Q_{in,N_Z}(t) \\ T_{out}(t) \\ I_T(t) \end{bmatrix} \tag{9}$$

with

$$I_{T,z} = I_b \cdot R_b + I_d \cdot \left(\frac{1 + cos\beta_z}{2}\right) + I \cdot p_g \cdot \left(\frac{1 - cos\beta_z}{2}\right) \tag{10}$$

$$R_b = \frac{cos\theta}{cos\theta_z} \tag{11}$$

The elements of the matrix $\boldsymbol{A_b}$ with dimension $(N_Z \times N_Z)$ are calculated in (12)-(13).

$$A_{j,j} = -\sum_{y \in \mathcal{E}} U_{wall,y} \cdot F_{wall,y} - \sum_{x \in \mathcal{J}} U_{wall,x} \cdot F_{wall,x} - \frac{1}{p_z \cdot C_z \cdot V_z} \cdot \sum_{y \in \mathcal{E}} U_{win,y} \cdot F_{win,y} \tag{12}$$

$$A_{j,i} = \begin{cases} \dfrac{1}{p_z \cdot C_z \cdot V_z} \cdot U_{wall,x} \cdot F_{wall,x}, & j, i \in \mathcal{N} \\ 0, & j, i \notin \mathcal{N} \end{cases} \tag{13}$$

The dimension of $\boldsymbol{B_b}$ is $N_Z \times (2N_Z + 2)$ and it is calculated as in the following,

$$\boldsymbol{B_b} = \frac{1}{p_z \cdot C_z \cdot V_z}[-\mathbf{I}_{(N_Z \times N_Z)} \quad \mathbf{I}_{(N_Z \times N_Z)} \quad \boldsymbol{B_{ex,w}} \quad \boldsymbol{B_{rad}}] \tag{14}$$

with

$$\boldsymbol{B_{ex,w}}_{(N_Z \times 1)} = \begin{bmatrix} B_{ex,w,1} \\ \vdots \\ B_{ex,w,N_Z} \end{bmatrix} \tag{15}$$

$$\boldsymbol{B_{rad}}_{(N_Z \times 1)} = \begin{bmatrix} B_{rad,1} \\ \vdots \\ B_{rad,N_Z} \end{bmatrix} \tag{16}$$

The elements of the submatrices $\boldsymbol{B_{ex,w}}$ and $\boldsymbol{B_{rad}}$ of matrix $\boldsymbol{B_b}$ are determined as it follows.

$$B_{ex,w,z} = \sum_{y \in \mathcal{E}} U_{wall,y} \cdot F_{wall,y} + \sum_{y \in \mathcal{E}} U_{win,y} \cdot F_{win,y} \tag{17}$$

$$B_{rad,z} = \sum_{y \in \mathcal{E}} a_w \cdot R_{se} \cdot U_{wall,y} \cdot F_{wall,y} + \sum_{y \in \mathcal{E}} \tau_{win} \cdot SC \cdot F_{win,y} \tag{18}$$

Considering as output the internal temperatures of the thermal zones then the matrices $\boldsymbol{C_b}$ and $\boldsymbol{D_b}$ are defined as in the following,

$$\boldsymbol{C_b}_{(N_Z \times N_Z)} = \mathbf{I}_{(N_Z \times N_Z)} \tag{19}$$

$$\boldsymbol{D_b}_{(N_Z \times 2N_Z+2)} = \mathbf{0}_{(N_Z \times 2N_Z+2)} \tag{20}$$

The system of continuous time equations (7)-(8) is converted to discrete time equations (21)-(22).

$$\boldsymbol{T_{in}}(k+1) = \boldsymbol{A_{b,d}} \cdot \boldsymbol{T_{in}}(k) + \boldsymbol{B_{b,d}} \cdot \boldsymbol{U} \tag{21}$$

$$\boldsymbol{Y}(k) = \boldsymbol{C_{b,d}} \cdot \boldsymbol{T_{in}}(k) + \boldsymbol{D_{b,d}} \cdot \boldsymbol{U} \tag{22}$$

3.2 Smart Power Dispatch Technique

A straightforward method is employed to allocate the building's total thermal power needs to its individual thermal zones. The amount of thermal power needed for each zone is determined based on the building's overall thermal power requirements, the volume of each thermal zone, and the estimated internal temperature along with its maximum and minimum limits. This approach minimizes computation time by first optimizing the total thermal power for the building and then distributing it across the thermal zones.

Advanced power dispatch methods are used to determine the power set-points for individual components, such as thermal zones. This process involves leveraging a novel approach to define the flexibility of thermal zones in adjusting the active power of their HVAC systems.

The estimated indoor temperature of a thermal zone, along with its maximum and minimum bounds, is utilized to accurately define how each thermal zone in a building can adjust its thermal power requirements, as illustrated by the following equations.

$$FL_z^{\uparrow}(t) = \frac{T_{in,z}(t) - T_{min,z}}{T_{max,z} - T_{min,z}} \tag{23}$$

$$FL_z^{\downarrow}(t) = \frac{T_{max,z} - T_{in,z}(t)}{T_{max,z} - T_{min,z}} \tag{24}$$

The total building's HVAC electric consumption is dispatched to its thermal zones according to Equation (25).

$$P_{HVAC,z}(t) = \frac{FL_z(t) \cdot V_z}{\sum_z \{FL_z(t) \cdot V_z\}} \cdot P_{HVAC,b}(t) \tag{25}$$

3.3 Building Thermal Load Constraints

$$T_{min,z} \leq T_{in,z}(t) \leq T_{max,z} \tag{26}$$

$$P_{HVAC,b,min} \leq P_{HVAC,b}(t) \leq P_{HVAC,b,max} \tag{27}$$

$$P_{HVAC,z,min} \leq P_{HVAC,z}(t) \leq P_{HVAC,z,max} \tag{28}$$

$$\sum_z P_{HVAC,z}(t) = P_{HVAC,b}(t) \tag{29}$$

$$P_{HVAC,z} = \frac{Q_{HVAC,z}}{COP}, \quad P_{HVAC,b} = \frac{Q_{HVAC,b}}{COP} \tag{30}$$

Chapter 4

System Identification, Particle Swarm Optimization and Clustering Overview

4.1 System Identification

System identification is a technique used to create mathematical models of dynamic systems based on measurements of their input and output signals. This process involves recording these signals, choosing an appropriate model structure, applying an estimation method to determine the values for the model's adjustable parameters, and then assessing the model to ensure it meets the requirements for the intended application [25]-[29].

There are three types of problems in the field of system identification, as shown in Figure 1:

1. ***White Box Model***, in which we have physical knowledge of the system.
2. ***Grey Box Model***, in which, despite not having precise knowledge of the internal workings of the system, a model is developed based on both understanding of the system and experimental data.
3. ***Black Box Model***, in which we don't have any knowledge of what's going on inside the system.

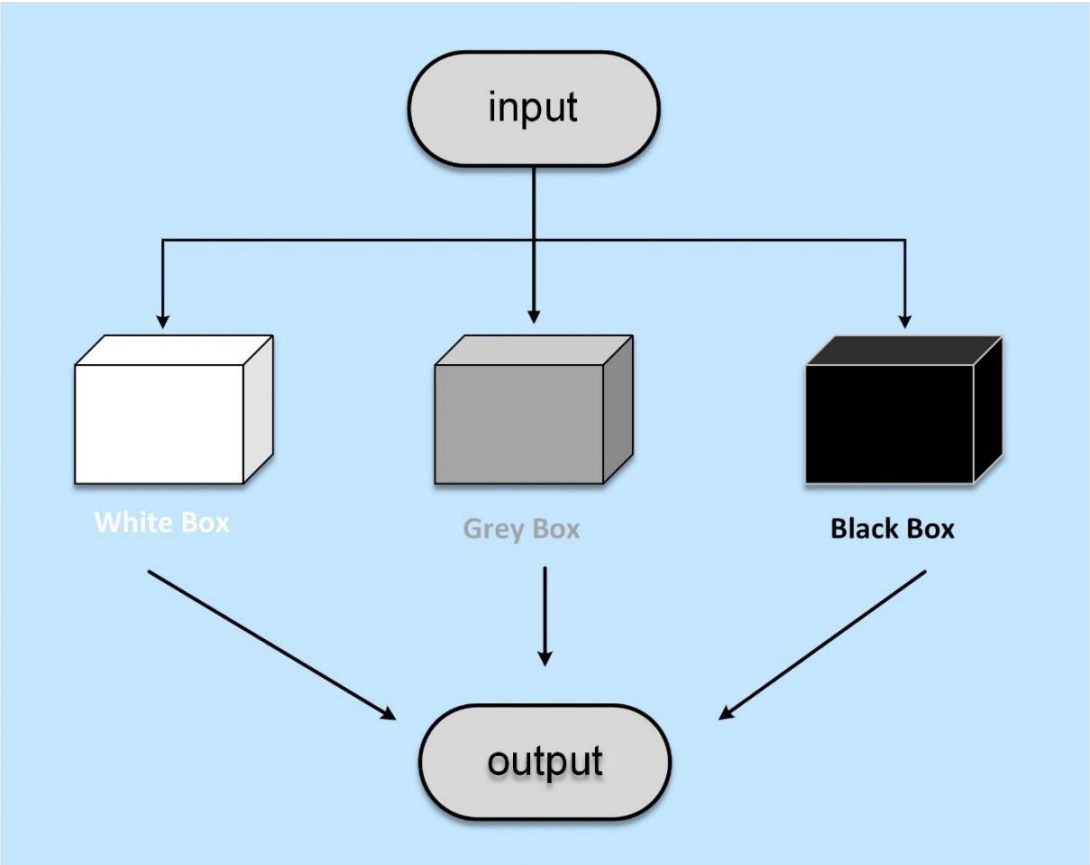

Figure 1. Types of models in the field of system identification

In this case, a system with unknown dynamics is present and a model is desired to make predictions about how the system will behave in the future (Black Box approach). The input and output data can be used to extract a model that mimics the connection between them.

Model is a mathematical description of the dynamic behavior of the system or process in either the time or frequency domain. In simple terms, model is a simplified representation of a real system. Different models can be used in *System identification*, such as Linear Models, Nonlinear Models or even Online and Recursive Models.

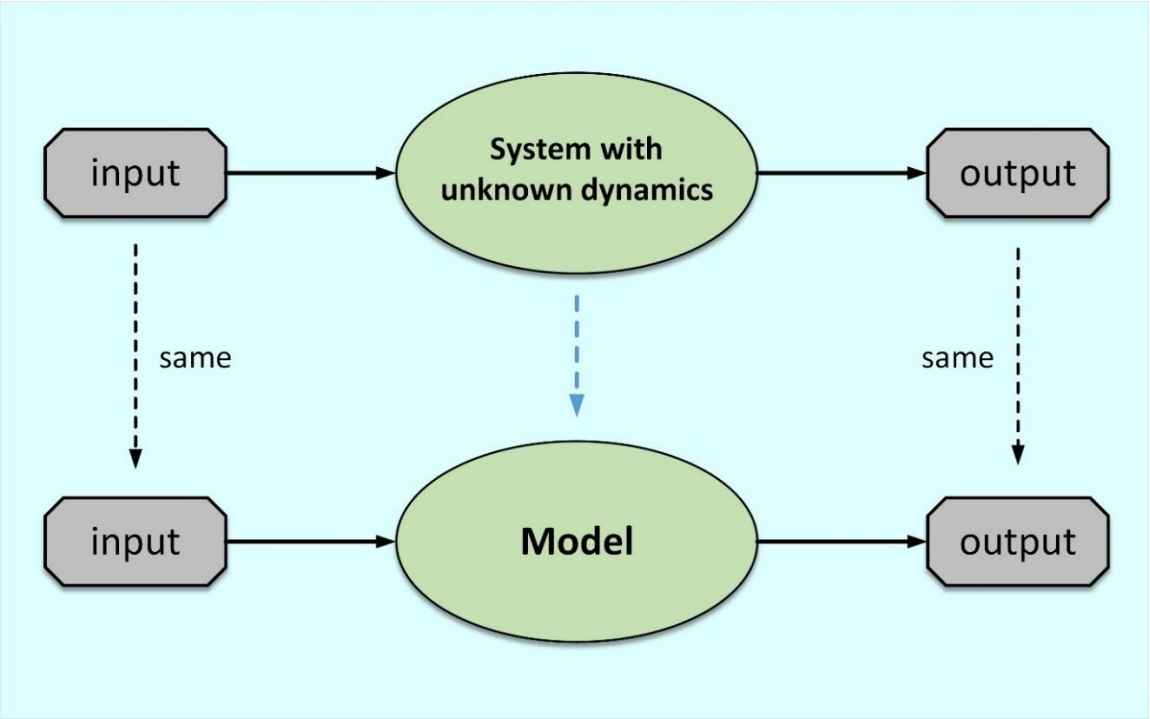

Figure 2. Relation between system and model

Another method that could be used to predict what the system output would be in the future is Curve Fit. In this situation, a curve is fitted to the data and extended into the future. The structure of the curve equation is picked, and it is then fitted to the data by adjusting the parameters. However, the underlying mechanisms that created the data are not described by Curve Fitting. For example, no prediction of what the output would be if the system were initialized in a different state or given different input data is provided by Curve Fit.

On the other hand, with System Identification, the core relation between the values of the data is taken advantage of to fit a dynamic model to it. A model is built whose output isn't just a function of time but is also a function of the previous system values. This model can then be used to predict what the data would look like from different starting conditions and with different input values.

A model structure that is thought to represent the behavior of the system must be chosen and fitted to the data, knowing that the system is nonlinear. The following model structures can be used:

- Nonlinear ARX
- Hammerstein – Wiener
- Neural Network

All of these will be fitted to our data to see which best suits our needs (best fit – trial and error process).

4.1.1 Nonlinear ARX

The design of these models allows for the representation of intricate nonlinear behaviors through adaptable nonlinear functions like wavelet and sigmoid networks [30]. For instance, a linear SISO (single input–single output) ARX model is structured as follows:

$$y(t) + a_1 \cdot y(t-1) + a_2 \cdot y(t-2) + \cdots + a_{na} \cdot y(t-na) = \\ = b_1 \cdot u(t) + b_2 \cdot u(t-1) + \cdots + b_n \cdot u(t-nb+1) + e(t) \quad (31)$$

- **u**: input
- **y**: output
- **e**: noise
- **na**: number of past output terms
- **nb**: number of past input terms

Rewriting the equation as a product:

$$y_p = [-a_1, -a_2, \dots, -a_{na}, b_1, b_2, \dots, b_{nb}] * [y(t-1) \\ \cdot y(t-2), \dots, y(t-na), u(t), u(t-1), \dots, u(t-nb+1)] \quad (32)$$

- $y(t-1), y(t-2), \dots, y(t-na)$, $u(t)$, $u(t-1)$, … , $u(t-nb+1)$: delayed input and output variables called *regressors*.
- $[a_1$, …, $b_{nb}]$: the coefficients vector represents the weighting applied to these regressors.

The linear ARX modes predicts the current output y_p as a weighted sum of its regressors.

Instead of the weighted sum of the regressors, the nonlinear ARX model has a more flexible nonlinear function F, where inputs to F are model regressors.

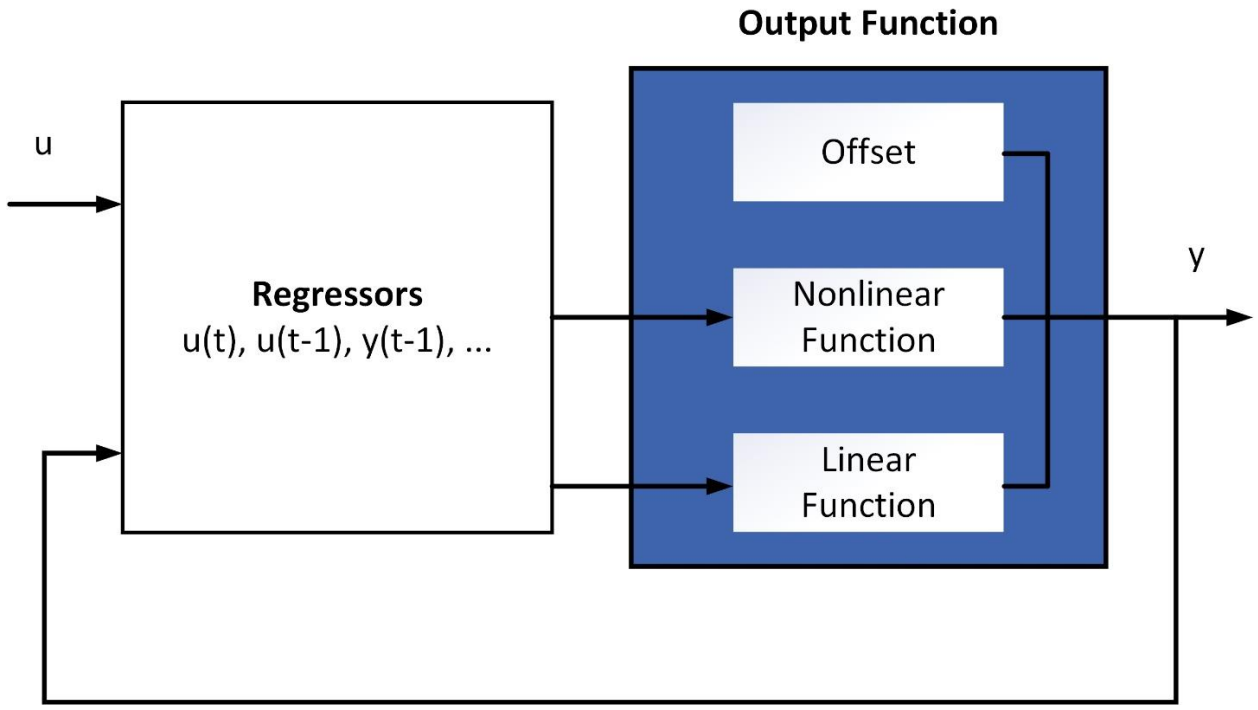

Figure 3. Nonlinear ARX Model

$$y_p(t) = F(y(t-1), y(t-2), y(t-3), \dots, u(t), u(t-1), u(t-2), \dots) \quad (33)$$

F can represent a weighted sum of several available nonlinear functions, that operate on the distance of the regressors from their means.

4.1.2 Hammerstein – Wiener

When a system's output is influenced nonlinearly by its inputs, it is occasionally feasible to break down the input-output relationship into multiple interconnected components. The *Hammerstein-Wiener* model accomplishes this by connecting static nonlinear blocks in series with a dynamic linear block. This model offers a straightforward block representation, maintains a clear connection to linear systems, and is more user-friendly compared to more complex nonlinear models like neural networks and Volterra models [31].

The following diagram represents the structure of *Hammerstein – Wiener* model:

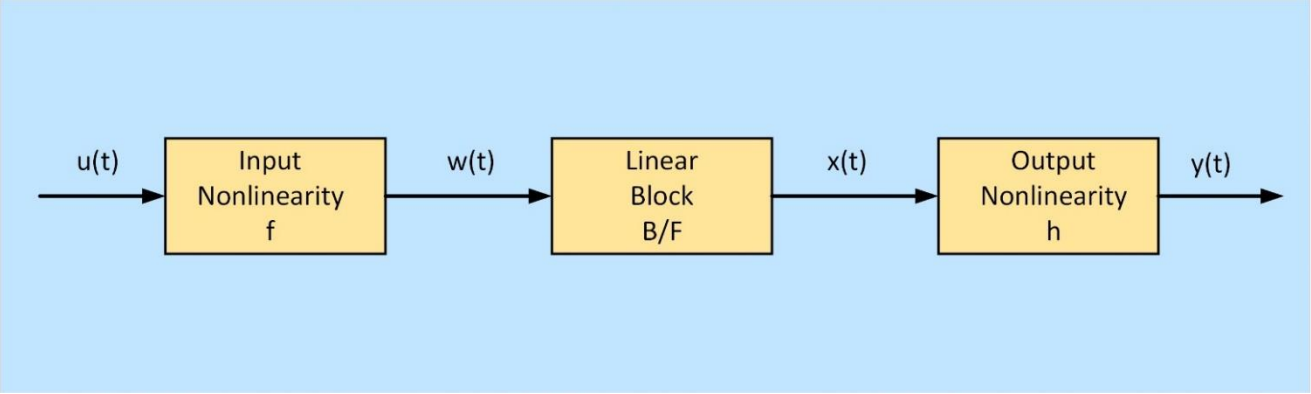

Figure 4. Hammerstein – Wiener Model

- $\boldsymbol{f}$: nonlinear function that transforms input data $u(t)$ as $w(t) = f\big(u(t)\big)$.
- **B/F**: linear transfer function that transforms $w(t)$ as $x(t) = B/F \cdot w(t)$.
- $\boldsymbol{h}$: nonlinear function that maps the output of the linear block $x(t)$ to the system output $y(t)$ as $y(t) = h(x(t))$.

4.1.3 Neural Networks

A Neural Network is a computational model inspired by the architecture and operations of biological neural networks found in the human brain. It consists of interconnected units known as neurons, analogous to brain neurons, linked by connections that simulate synapses. Each neuron processes incoming signals from connected neurons and transmits a signal to other neurons. This signal is a numerical value, and each neuron's output is derived from a nonlinear function applied to the sum of its inputs, referred to as the activation function. The connection strength, or weight, is adjusted throughout the learning process. Neural Networks are particularly effective for modeling nonlinear relationships and are commonly used in tasks like pattern recognition, object classification, and control systems [32]-[34].

Generally, neurons are separated into layers. The first layer represents the inputs and the last layer the outputs. Between these two, there are one or more hidden layers, each one of them may perform different transformations on their inputs. Neural Networks can be trained using many examples to recognize patterns and it adjusts the weights according to a specified learning rule, until it performs the desired task correctly.

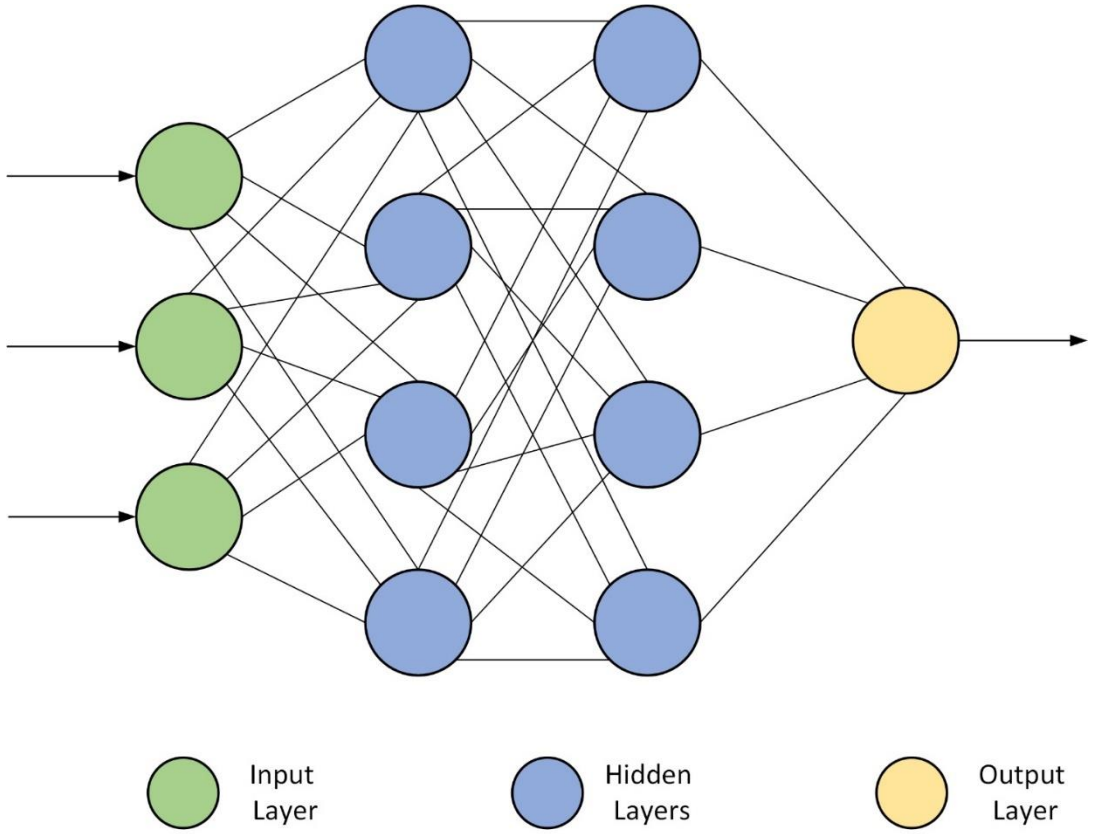

Figure 5. Neural Network Model

4.2 Particle Swarm Optimization

Particle Swarm Optimization (PSO) is an advanced optimization technique rooted in Swarm Intelligence principles [35]. Known for its high efficiency and straightforward implementation, PSO is a powerful heuristic method. It has demonstrated significant robustness and effectiveness in tackling complex optimization challenges. Unlike traditional methods, PSO is less sensitive to the initial point and tends to converge to a global optimum with a high success rate. Classical methods often struggle to find the global optimum in high-dimensional optimization problems and with very complex objective functions.

PSO involves a group of potential solutions known as a swarm of particles. Each particle occupies a position within the optimization problem's search space. This search space encompasses all possible solutions to the problem, and the goal is to identify the optimal one.

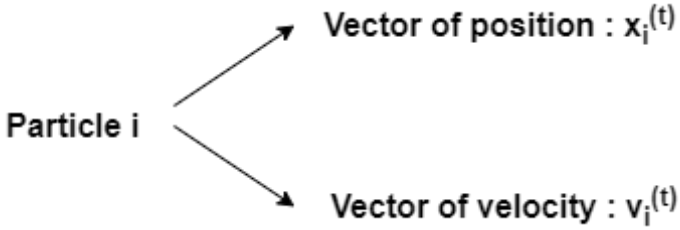

- $x_i^{(t)} \in X$: Describes the position of the particle i in the search space X.
- $v_i^{(t)} \in X$: Describes the movement of the particle i in the sense of direction and distance. It is in the same space as the position. Dimensions of v and x are the same.
- t : discrete time expressing the iteration number of the algorithm.

  A classic PSO method can be described as in the following:

- $v_i^{(t+1)} = w \cdot v_i^{(t)} + c_1 \cdot r_1 \cdot \left(P_i - x_i^{(t)}\right) + c_2 \cdot r_2 \cdot \left(G - x_i^{(t)}\right)$

- $x_i^{(t+1)} = x_i^{(t)} + v_i^{(t+1)}$

❖ P_i : the best previous solution corresponding to the i^{th} particle
❖ G : the best global solution
❖ w : the inertia weight factor
❖ c_1, c_2 : acceleration constants
❖ r_1, r_2 : random numbers varying between 0 and 1

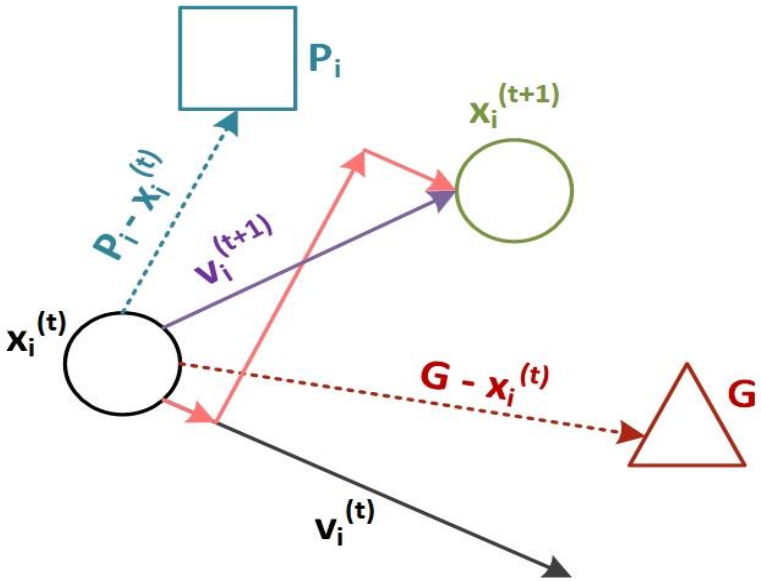

Figure 6. Particles Iteration

4.3 Theoretical Background of K-means Clustering

K-means clustering is a widely used algorithm in unsupervised machine learning for partitioning a dataset into K distinct, non-overlapping clusters. The goal is to organize the data into clusters where data points within each cluster are more similar to each other than to those in other clusters. The aim of using K-means clustering is to uncover and understand the natural groupings within a dataset. By partitioning the data into clusters, it helps in simplifying data analysis, enhancing data interpretation, optimizing resources, detecting anomalies, and supporting informed decision-making across various domains.

The objective function can be expressed mathematically as:

$$J = \sum_{i=1}^{K} \sum_{x \in C_i} \|x - \mu_i\|^2$$

where

- K is the number of clusters.
- C_i is the set of points in cluster i
- μ_i is the centroid of cluster i
- $\|x - \mu_i\|^2$ is the Euclidean distance between point x and centroid μ_i

The k-means algorithm follows a simple yet iterative approach to achieve the objective:

1. Initialization: Randomly select K initial centroids from the dataset. This can significantly affect the final results, hence strategies like K-means++ are often used to select better initial centroids.

2. Assignment: Assign each data point to the nearest centroid. This forms ***K*** clusters based on the minimum Euclidean distance to the centroids.

3. Update: Recalculate the centroids of the clusters. The new centroid of each cluster is the mean of all points assigned to that cluster.

4. Convergence: Repeat the assignment and update steps until the centroids no longer change significantly or the maximum number of iterations is reached. Convergence is typically determined when the changes in centroids fall below a specified threshold.

Chapter 5

Control of Building Energy Systems using System Identification

5.1 Problem Formulation

In this chapter, we aim to develop an accurate model for estimating the indoor temperature of building thermal zones, which is a critical aspect of energy management and occupant comfort. The model utilizes four key inputs: the internal thermal loads within the thermal zones, which encompass heat generated by occupants, lighting, and equipment; the power consumption of the HVAC system responsible for regulating the indoor climate; the ambient temperature, which influences the thermal balance between the building and its environment; and solar irradiation, which impacts the indoor temperature through direct and indirect heating. To achieve this, we apply advanced modeling techniques, specifically system identification and neural networks. System identification involves creating mathematical models based on observed data to capture the dynamic behavior of the thermal zones, while neural networks offer a data-driven approach to learn complex, nonlinear relationships between the inputs and the indoor temperature. By developing and validating these models, we aim to enhance the efficiency of HVAC systems, reduce energy consumption, and improve thermal comfort within buildings, contributing to more sustainable and cost-effective building management practices.

5.2 Case Study

In the analyzed case study, the energy system under investigation includes a large-scale office building.

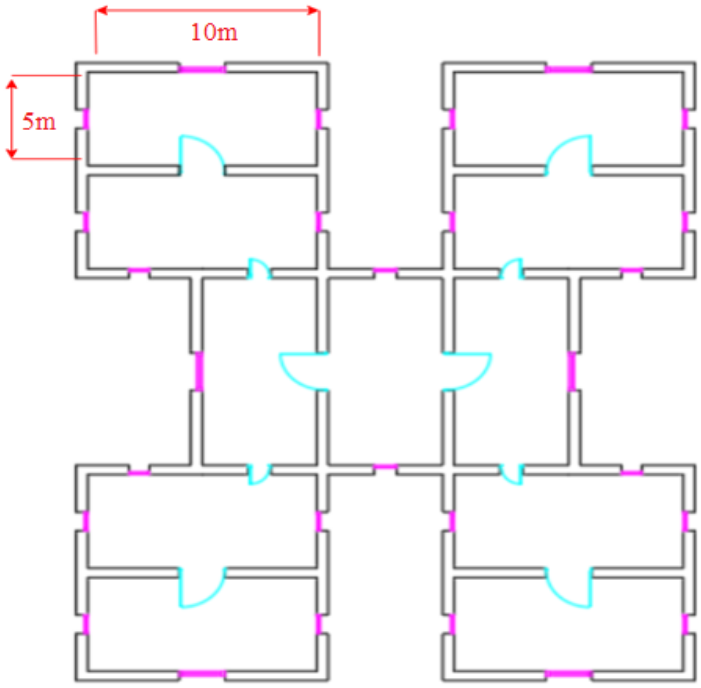

Figure 7. Floor plan (10 floors, 11 thermal zones per floor)

The floor plan is depicted in Figure 7. Table 1 outlines the model characteristics pertinent to the thermal zones. Figure 8 illustrates the time series data for ambient temperature and solar radiation levels.

Table 1. Thermal zones characteristics

THERMAL ZONES MODELLING DATA					
$p_z(kg/m^3)$	1.2	$\tau_{win,}$	$1.1 \cdot 10^{-3}$	$\beta_z(°)$	90
$C_z(kWh/(kg \cdot °C))$	1/3600	$a_{w,z}$	$18.6 \cdot 10^{-3}$	$\theta(°)$	11.9
$U_{wall,z}(kW/(m^2 \cdot °C))$	$2.04 \cdot 10^{-3}$	SC_z	0.54	$\theta_z(°)$	39.9
$U_{win,z}(kW/(m^2 \cdot °C))$	$5.6 \cdot 10^{-3}$	p_g	0.2	$R_{se,z}((m^2 \cdot °C)/kW)$	40

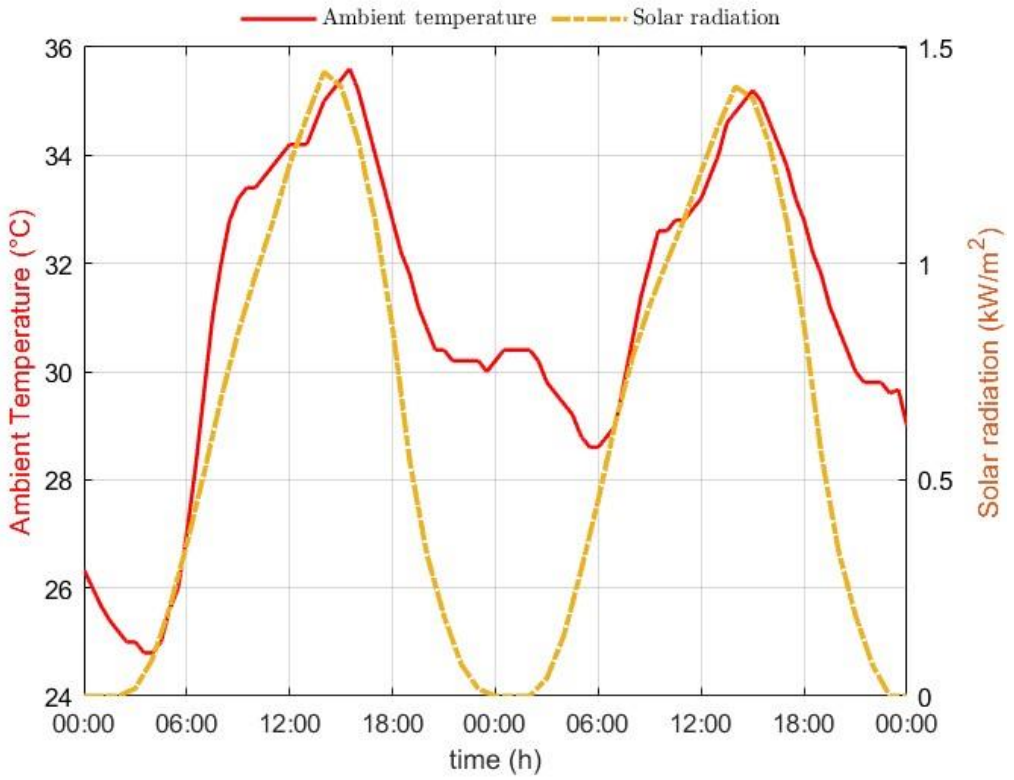

Figure 8. Ambient temperature and irradiation

Using K-means clustering on indoor temperature data, $T_{in,z}$, of building thermal zones aims to classify these zones into 4 clusters with similar temperature patterns. The objectives of applying **k-means clustering** to indoor temperature data are the following:

1. **Identify Temperature Patterns**: The primary objective is to identify and group similar temperature patterns within the building's thermal zones. Each cluster will represent a set of thermal zones that exhibit similar temperature behaviors.
2. **Characterize Different Thermal Zones**: By clustering the temperature data, we can characterize different types of thermal zones within the building. For example, some clusters might correspond to rooms that are generally warmer, cooler, or have more stable temperatures.

3. **Optimize Energy Usage:** Understanding these clusters can help in optimizing HVAC systems. By recognizing zones with similar temperature profiles, the HVAC system can be more efficiently managed to maintain desired temperatures, potentially leading to energy savings.

When we use $[\boldsymbol{idx}, \boldsymbol{C}] = \boldsymbol{kmeans}(\boldsymbol{Tin\_z}, \boldsymbol{4})$; in the context where Tin_z represents the indoor temperature data of different building thermal zones, we are applying the k-means clustering algorithm to partition these temperature readings into 4 distinct clusters. "$\boldsymbol{idx}$"($\boldsymbol{Cluster\ Indices}$) is a vector that contains the cluster index for each temperature data point in Tin_z. Each element in idx corresponds to a thermal zone and indicates which of the 4 clusters it belongs to. For instance, if idx (1) = 2, it means that the first thermal zone is assigned to the second cluster. "$\boldsymbol{C}$" is a matrix where each row represents the centroid (average temperature profile) of one of the 4 clusters. These centroids are the mean temperature profiles of the thermal zones assigned to each cluster. The centroid provides a summary of the typical temperature pattern for each cluster. The results obtained by applying the clustering of thermal zones for internal thermal gains, power of HVAC systems and internal temperatures of the building thermal zones are given below.

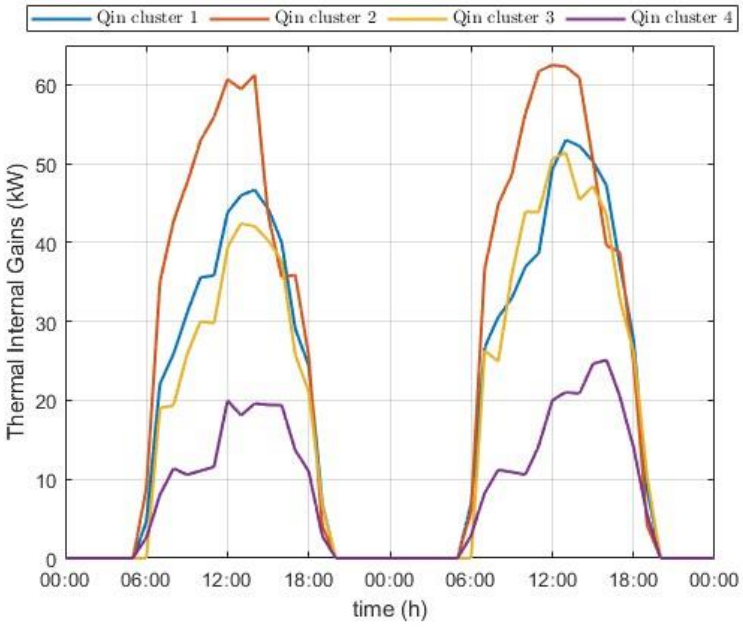

Figure 9. Internal thermal gains of 4 clusters

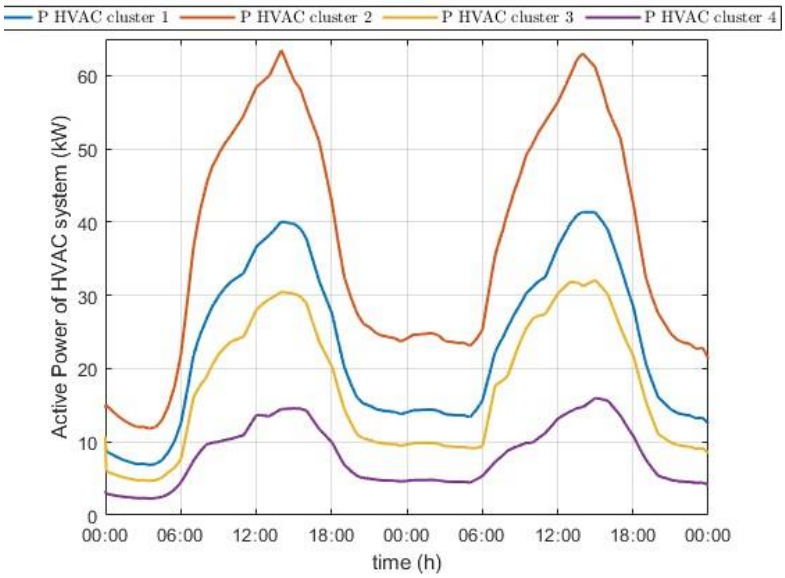

Figure 10. Active power of HVAC system of 4 clusters

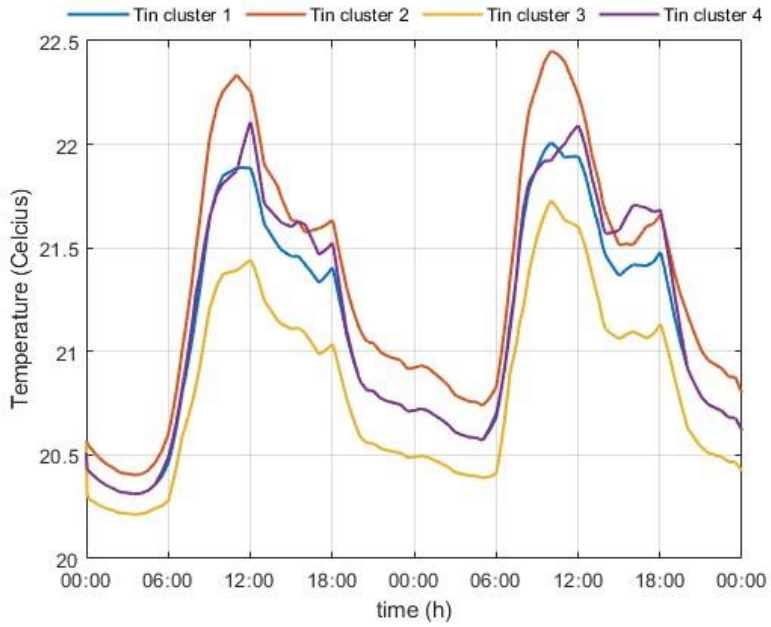

Figure 11. Indoor temperature of 4 clusters

5.3 Results

As mentioned previously, three model structures can be utilized to represent the behavior of the nonlinear system and fit it to the data. These structures include the Nonlinear ARX, the Hammerstein-Wiener, and Neural Network models. Specific Matlab tools will be employed to determine which structure best meets our requirements. The System Identification Toolbox is being utilized for the first two structures, while the Neural Network Time Series Toolbox is being used for Neural Networks. This approach allows the use of Matlab's specialized environments, thus saving time and reducing the complexity of the problem-solving process.

The System Identification Toolbox facilitates learning the dynamic relationships among measured variables using either linear or nonlinear autoregressive modeling techniques. Subsequently, the steps taken to identify the structure that provides the best fit will be described.

5.3.1 Nonlinear ARX

First, the data (input and output) is loaded into the Matlab Workspace, and iddata objects are created to encapsulate both data values and data properties into a single entity. The iddata objects are then used to import the estimation and validation data. The creation of these objects is demonstrated below.

```
Ts = 360; % Sample time

% Cluster 1

id_1 = iddata(Cluster_1_Output_New,Cluster_1_Data_New,Ts);

id_1_est = id_1(1:2:end);

id_1_val = id_1(2:2:end);
```

Figure 12. Creation of iddata objects

The same process is applied to the other three clusters. This iddata is loaded into the System Identification Toolbox, where the sample time, input values, and output values are defined. The estimation and validation data are then loaded separately, as demonstrated below.

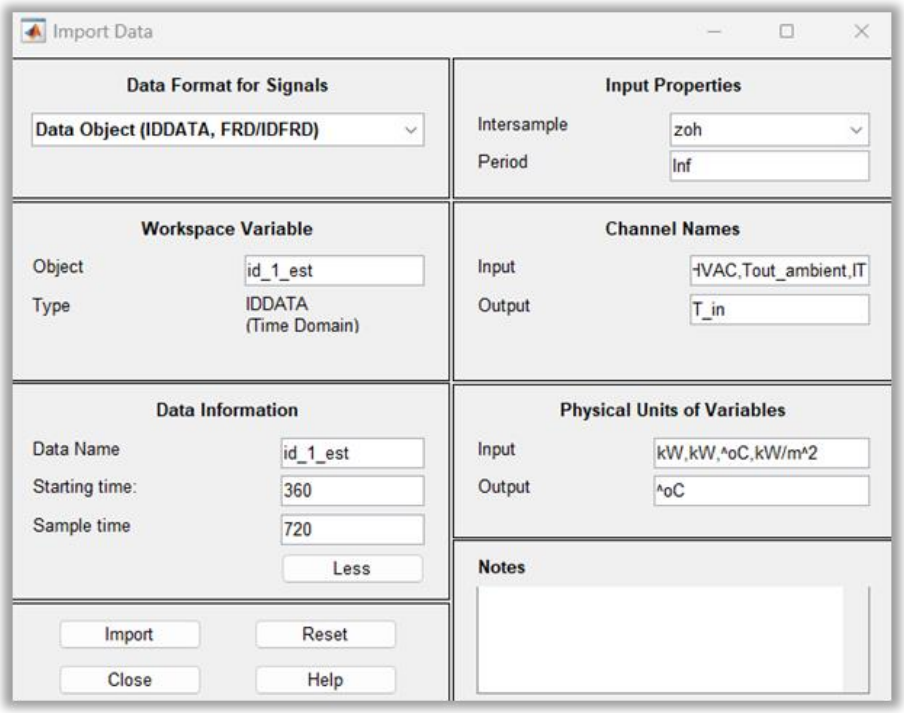

Figure 13. Estimation Data – Cluster 1

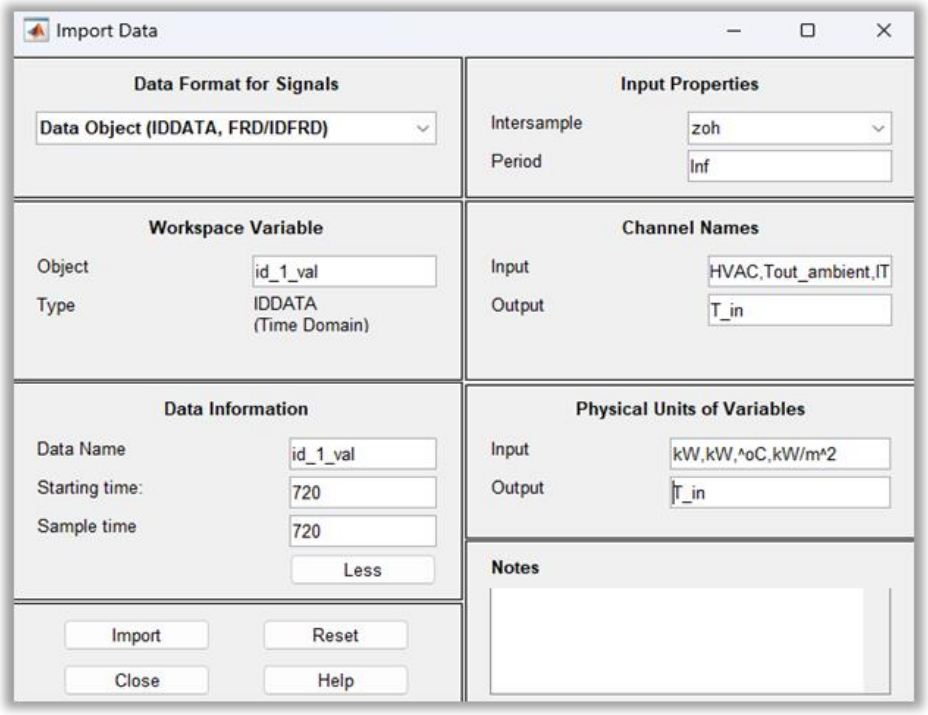

Figure 14. Validation Data – Cluster 1

The input variables are: $\boldsymbol{u_1 \rightarrow Q_{in}(kW), u_2 \rightarrow P_{HVAC}\,(kW), u_3 \rightarrow Tout_{ambient}(℃), u_4 \rightarrow IT(\frac{kW}{m^2})}$

The output variable is: $\boldsymbol{y \rightarrow T_{in}(℃)}$

Nonlinear ARX models are estimated using the default settings.

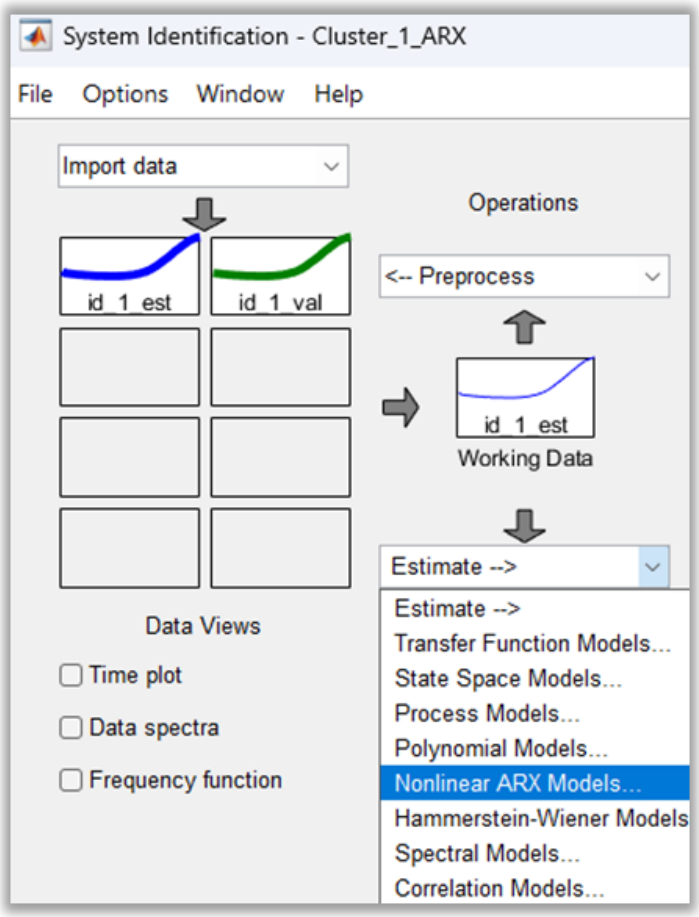

Figure 15. Nonlinear ARX model selection

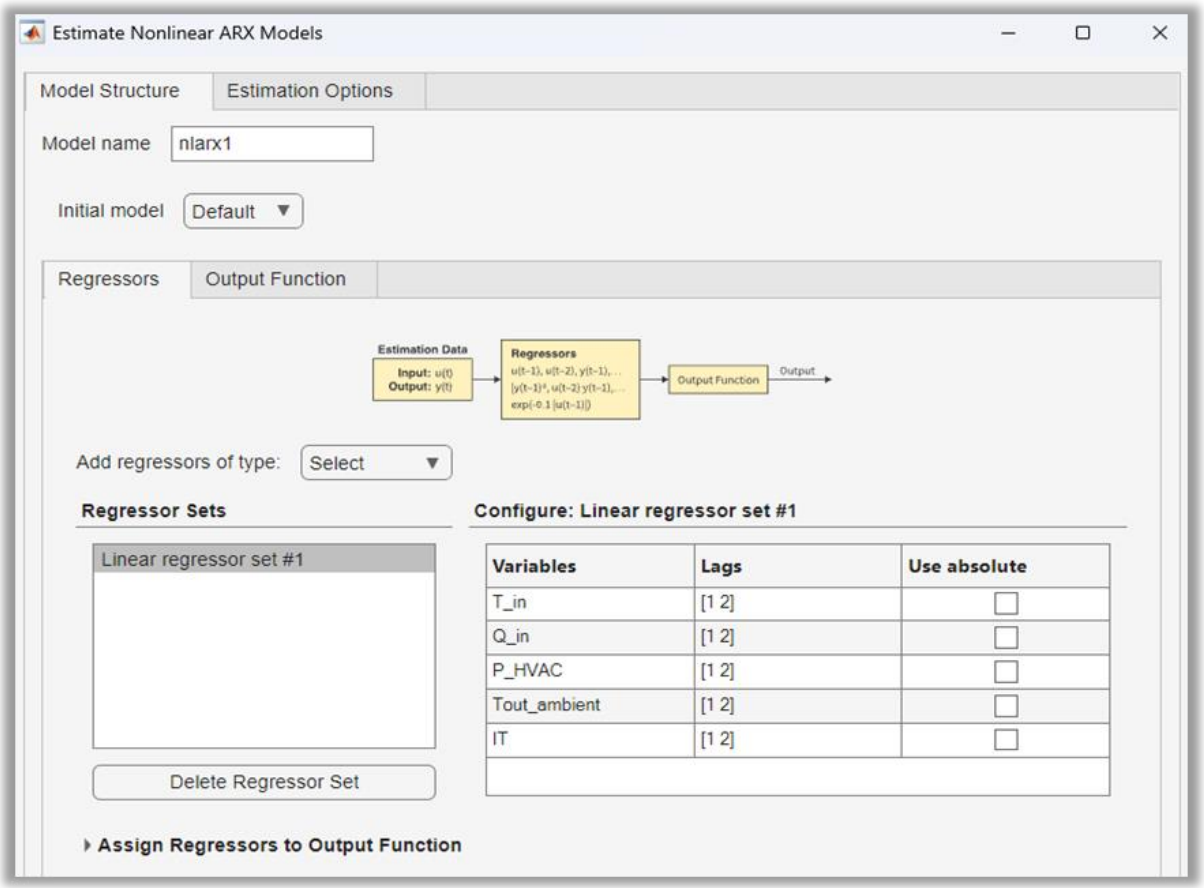

Figure 16. **Customization 1** (Linear Regressors, Linear Lags (Output))

Table 2. Customization 1 Results

Name	Linear Lags (Output)	Fit(%)
nlarx1	[1 2]	Nan
nlarx2	[2 3]	Nan
nlarx3	[3 4]	93,83
nlarx4	[4 5]	95,63
nlarx5	[5 6]	96,16
nlarx6	[6 7]	95,96
nlarx7	[7 8]	96,33
nlarx8	[8 9]	96,24

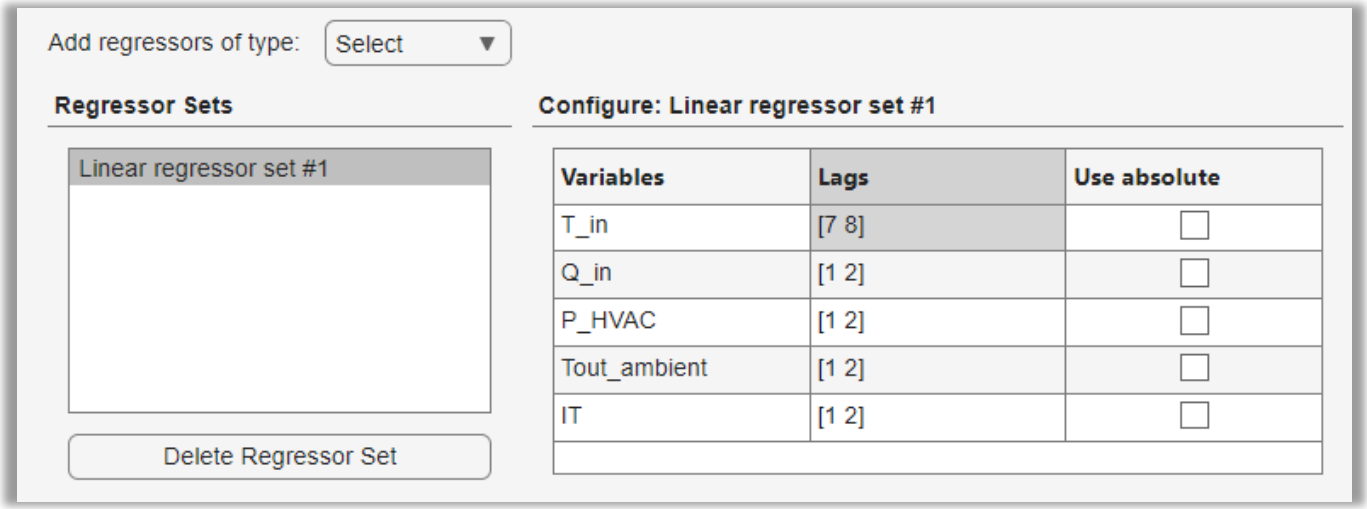

Figure 17. Example: $\boldsymbol{nlarx7 \rightarrow Lag\ T\_in = [7\ 8]}$

The model that has provided the best fit for our system so far is $\boldsymbol{nlarx7 = 96,33\%}$.

Customization 2 (Linear Regressors, Linear Output Lags = [7 8] , Polynomial Regressors , Polynomial Output Lags)

Table 3. Customization 2 Results

Name	Polynomial Lags (Output)	Fit(%)
nlarx9	[1 2]	94,29
nlarx10	[2 3]	94,40
nlarx11	[3 4]	94,56
nlarx12	[4 5]	94,57
nlarx13	[5 6]	94,56
nlarx14	[6 7]	94,80
nlarx15	[7 8]	95,16
nlarx16	[8 9]	95,02

The best model identified so far has not changed.

Customization 3 (Linear Regressors, Linear Output Lags = [7 8] , Periodic Regressors , Periodic Output Lags)

Table 4. Customization 3 Results

Name	Periodic Lags (Output)	Fit(%)
nlarx17	[1 2]	Nan
nlarx18	[2 3]	Nan
nlarx19	[3 4]	Nan
nlarx20	[4 5]	Nan

This customization leads to unacceptable fits, so the next option is pursued.

Customization 4 (Linear Regressors, Linear Output Lags = [7 8] , Polynomial Regressors , Polynomial Lags = [7 8] , Periodic Regressors , Periodic Lags)

Table 5. Customization 4 Results

Name	Periodic Lags (Output)	Fit(%)
nlarx21	[1 2]	Nan
nlarx22	[2 3]	Nan
nlarx23	[3 4]	Nan

This customization leads to unacceptable fits, so the next option is pursued.

Customization 5 (Linear Regressors, Linear Output Lags = [7 8] , Wavelet Network , Number of Units)

Table 6. Customization 5 Results

Name	Number of Units	Fit(%)
nlarx24	1	Nan
nlarx25	5	Nan
nlarx26	10	Nan
nlarx27	15	Nan

This customization leads to unacceptable fits, so the next option is pursued.

Customization 6 (Linear Regressors, Linear Lags = [7 8] , Sigmoid Network , Number of Units)

Table 7. Customization 6 Results

Name	Number of Units	Fit(%)
nlarx28	10	95,74
nlarx29	1	95,48
nlarx30	2	95,86
nlarx31	3	95,85
nlarx32	4	96,59
nlarx33	5	95,70
nlarx34	6	Nan
nlarx35	7	95,91
nlarx36	8	96,42
nlarx37	9	<95

nlarx38	11	95,86
nlarx39	12	96,15
nlarx40	13	<95

The new model that best fits our system so far is $nlarx32 = 96,59\%$.

Customization 7 (Linear Regressor, Linear Output Lags = [7 8] , Gaussian Process , Kernel function, Optimizer)

The last function used for the Nonlinear ARX structure is the Gaussian Process. In this scenario, two variables can be customized: the Kernel function and the optimizer. All possible combinations are presented in the following Table.

Table 8. Customization 7 Results

Kernel function	Optimizer
Exponential	Quasi-Newton
Squared Exponential	LBFGS-based quasi-Newton
Matern32	Simplex Search
Matern52	Unconstrained nonlinear optimization
Rational Quadratic	Interior-Point
ARD Exponential	Sequential Quadratic Programming
ARD Squared Exponential	-
ARD Matern32	-
ARD Matern52	-
ARD Rational Quadratic	-

Name	Kernel function	Optimizer	Fit(%)
nlarx41	Squared Exponential	Quasi-Newton	97,80
nlarx42	Squared Exponential	LBFGS	97,80
nlarx43	Squared Exponential	Simplex Search	97,80
nlarx44	Exponential	Quasi-Newton	98,45
nlarx45	Exponential	LBFGS	98,45
nlarx46	Matern32	Quasi-Newton	98,29
nlarx47	Matern52	Quasi-Newton	98,11
nlarx48	Rational Quadratic	Quasi-Newton	97,98

The model that best fits our system overall is $nlarx44 = 98,45\%$.

Further customization is not pursued because nearly every variable available for customization through Matlab Toolbox has been tried, and the overall fit is deemed satisfactory.

The results of the models extracted for the Nonlinear ARX structure for Cluster 1 are as follows. As observed from the above, **the model that best fits our system is the $nlarx44 = 98,45\%$**. This model corresponds to a combination of **Linear regressors with output lag = [7 8] and a Gaussian Process as the output function, with Exponential as the Kernel function and Quasi-Newton as the Optimizer**. Similar customizations have been applied to Clusters 2, 3, and 4, and their results are presented below.

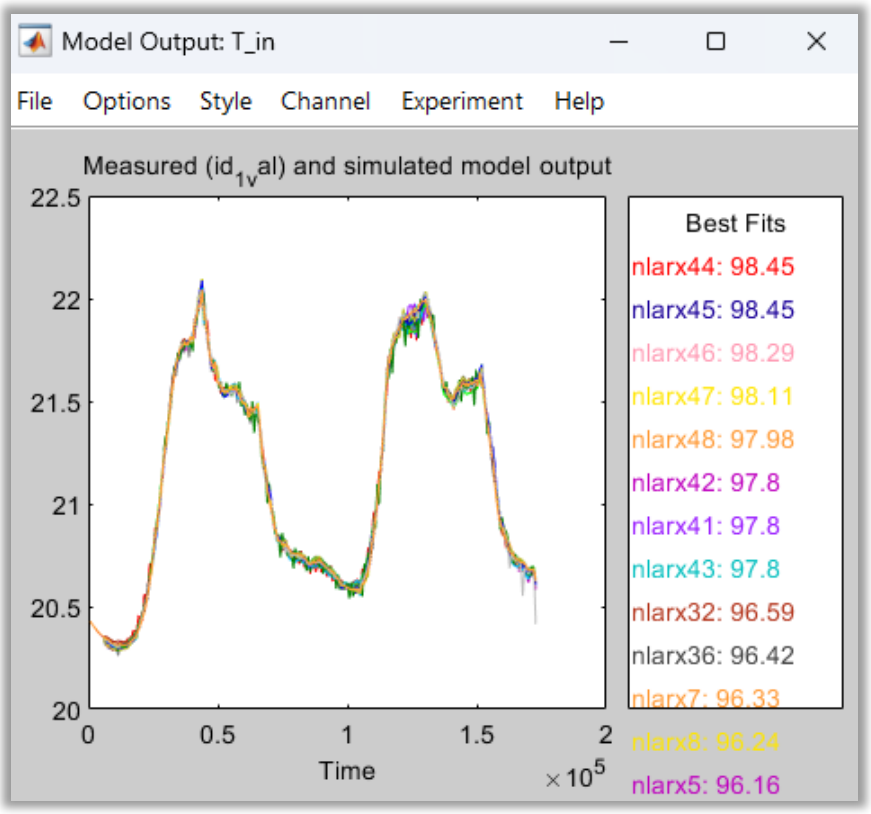

Figure 18. Results of the models extracted for the Nonlinear ARX structure for Cluster 1

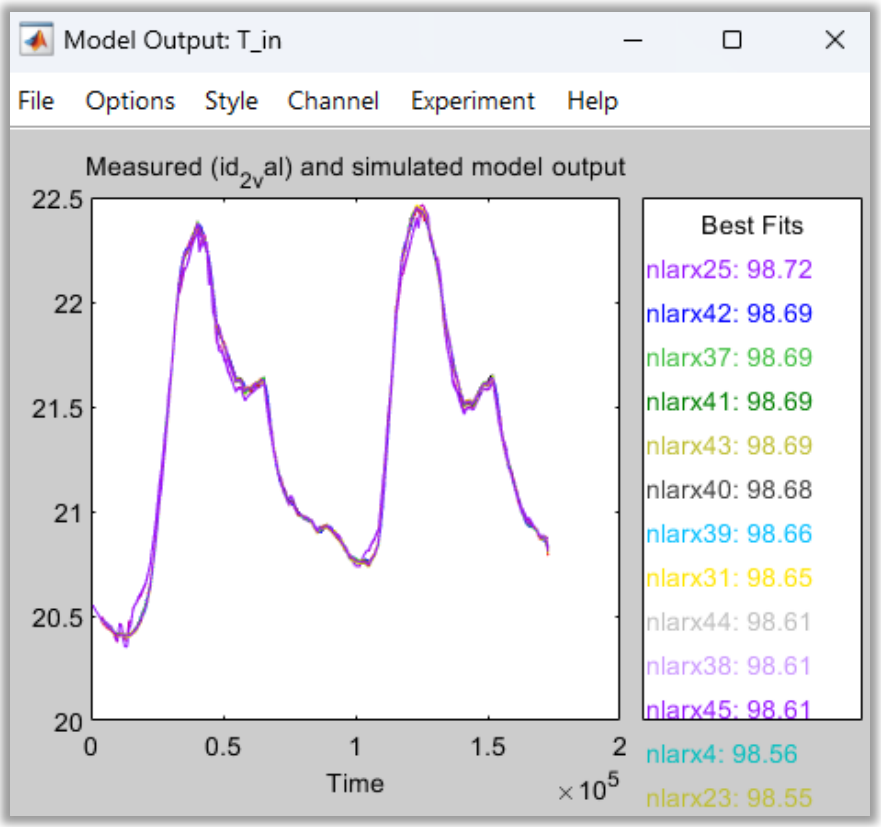

Figure 19. Results of the models extracted for the Nonlinear ARX structure for Cluster 2

As can be seen from the above, **the model that best fits our system is $nlarx25 = 98.72\%$**. This model consists solely of **Linear regressors with a linear output lag of [4 5]. The output function used is the Sigmoid Network with 4 units**.

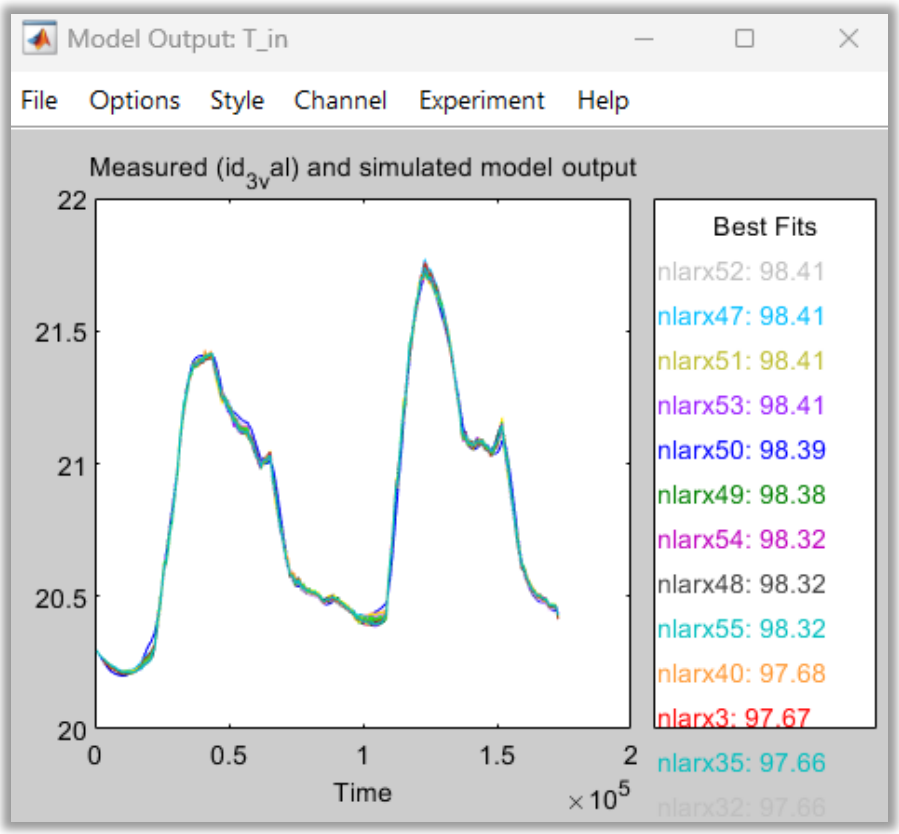

Figure 20. Results of the models extracted for the Nonlinear ARX structure for Cluster 3

As observed from the above, **the model that best fits our system is $nlarx52 = 98.41\%$**. This model comprises only **Linear regressors with a linear output lag of [3 4]. The output function utilized is the Gaussian Process, with the Squared Exponential as the Kernel function and LBFGS as the Optimizer.**

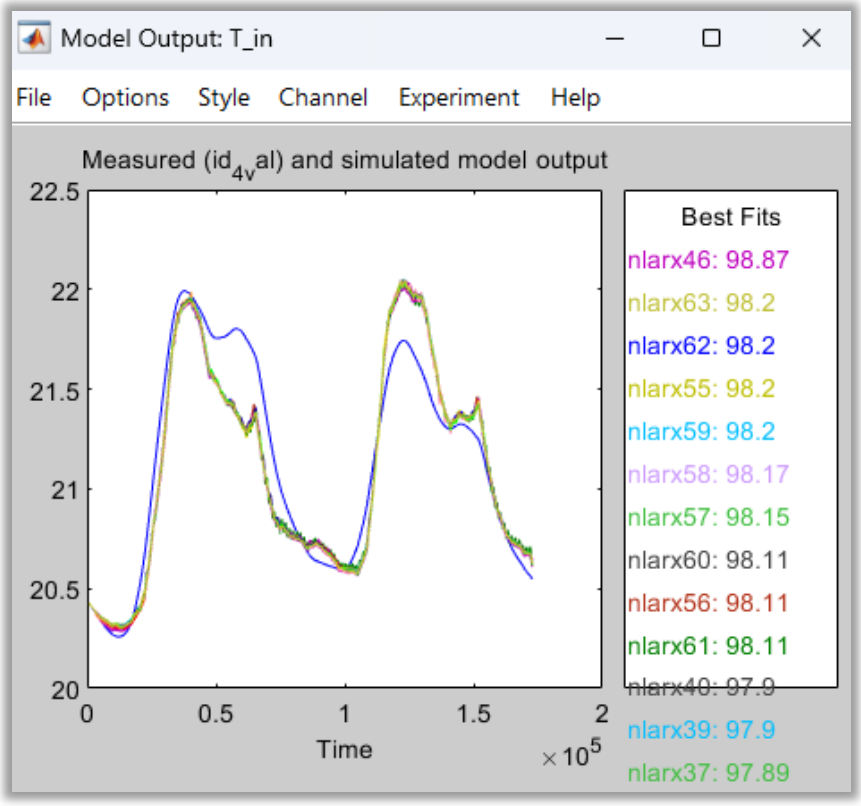

Figure 21. Results of the models extracted for the Nonlinear ARX structure for Cluster 4

As observed from the above, **the model that best fits our system is $nlarx46 = 98.87\%$**. This model includes only **Linear regressors with a linear output lag of [3 4]. The output function used is the Sigmoid Network with 3 units**.

5.3.2 Hammerstein-Wiener

The data (input and output) is loaded into the Matlab Workspace, and iddata objects are created. These iddata objects are used to import the estimation and validation data. This process is applied to each cluster. The iddata is then loaded into the System Identification Toolbox, where the sample time, input values, and output values are defined. The estimation and validation data are loaded separately.

All the above details were described and illustrated through figures for the Nonlinear ARX structure. Since the same details apply to the Hammerstein-Wiener structure, they will not be repeated. The input and output variables remain unchanged as well.

The input variables are: $u_1 \rightarrow Q_{in}(kW), u_2 \rightarrow P_{HVAC}(kW), u_3 \rightarrow Tout_{ambient}(^oC), u_4 \rightarrow IT(\frac{kW}{m^2})$

The output variable is: $T_{in}(^oC)$

Hammerstein-Wiener models are estimated using the default settings.

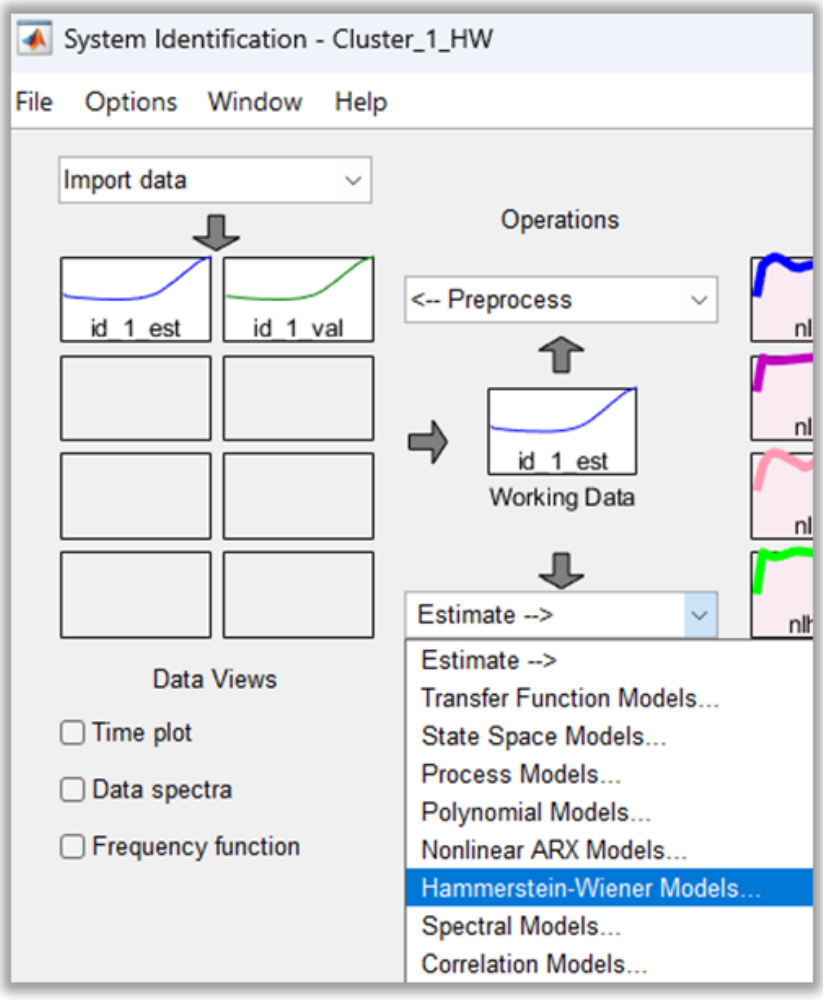

Figure 22. Hammerstein-Wiener model selection

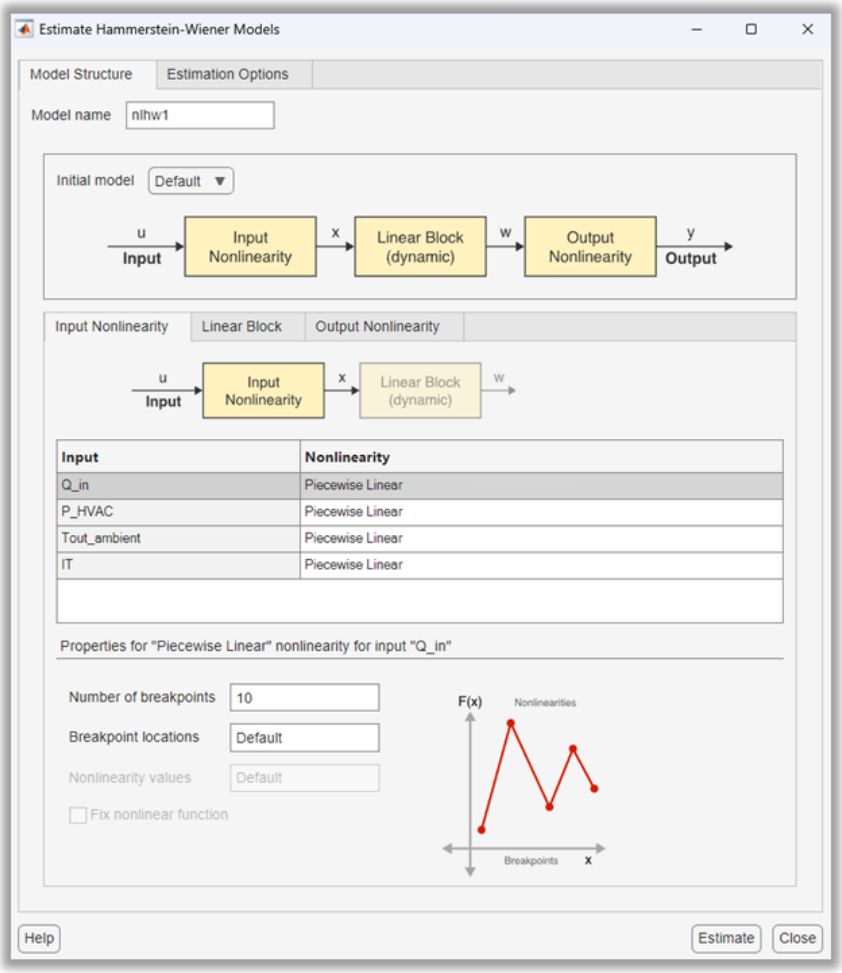

Figure 23a. Default structure of Hammerstein-Wiener model – a

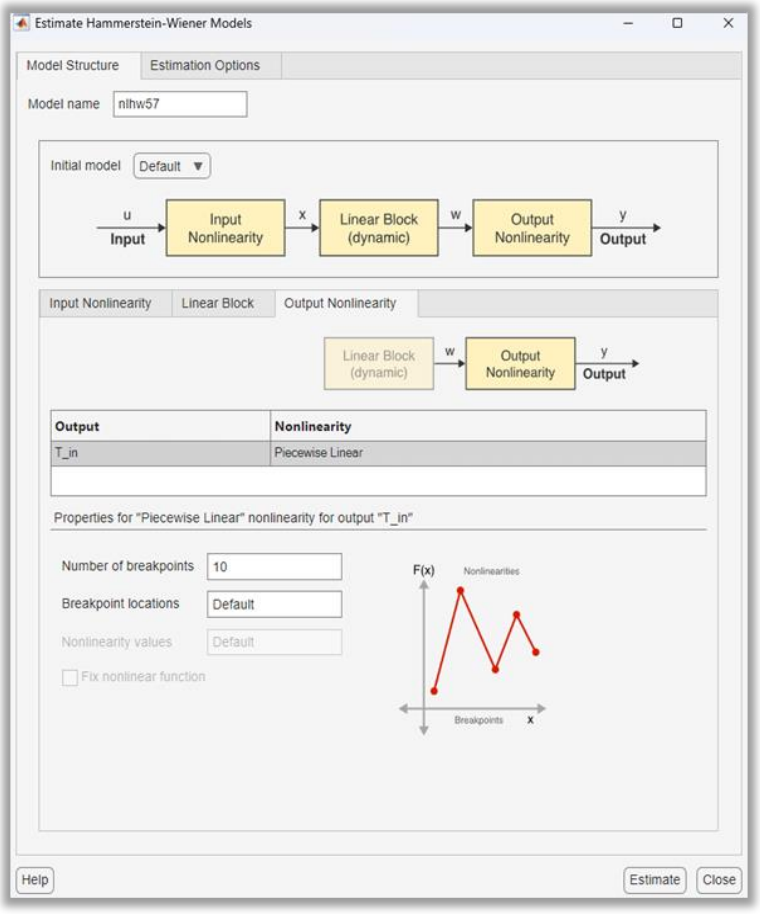

Figure 23b. Default structure of Hammerstein-Wiener model – b

Customization 1 (Input: Piecewise Linear, Input number of breakpoints = 10 , Output: Piecewise Linear , Output Number of Breakpoints)

Table 9. Customization 1 Results

Name	Number of Breakpoints (Output)	Fit(%)
nlhw1	10	95,33
nlhw2	1	55,48
nlhw3	2	93,88
nlhw4	3	95,39
nlhw5	4	95,46
nlhw6	5	95,32
nlhw7	6	88,66
nlhw8	7	95,37
nlhw9	8	93,47
nlhw10	9	95,37
nlhw11	11	95,36
nlhw12	15	92,82
nlhw13	20	79,55

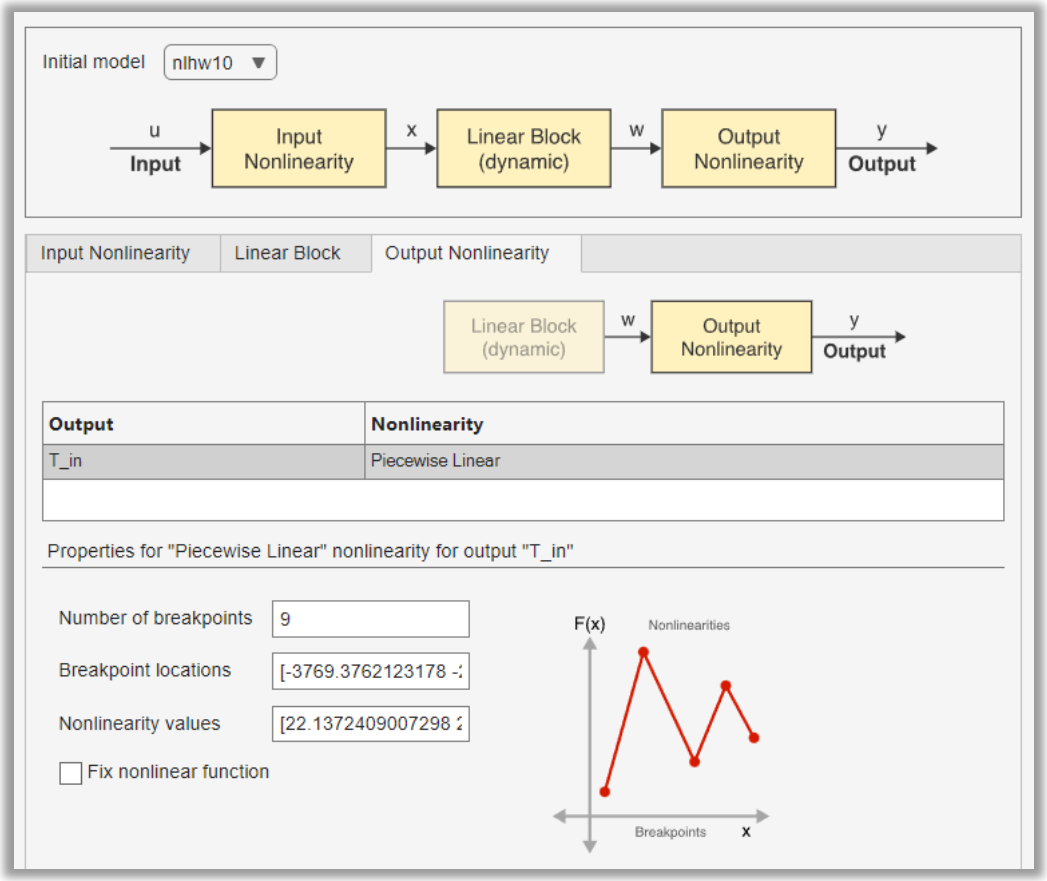

Figure 24. Example: $nlhw10 \rightarrow Number\ of\ breakpoints\ (Output) = 9$

The best fit so far is the $nlhw5 = 95,46\%$.

Customization 2 (Input: Piecewise Linear, Input number of breakpoints = 10 , Output: Sigmoid Network , Output Number of Units)

Table 10. Customization 2 Results

Name	Number of Units (Output)	Fit(%)
Nlhw14	10	95,35
Nlhw15	1	<90
Nlhw16	2	95,05
Nlhw17	3	95,56
Nlhw18	4	95,35
Nlhw19	5	91,21
Nlhw20	6	95,22
Nlhw21	7	95,88
Nlhw22	8	95,84
Nlhw23	9	91,58
Nlhw24	11	<90
Nlhw25	15	92,96
Nlhw26	20	95,60
Nlhw27	25	92,93
Nlhw28	30	92,16

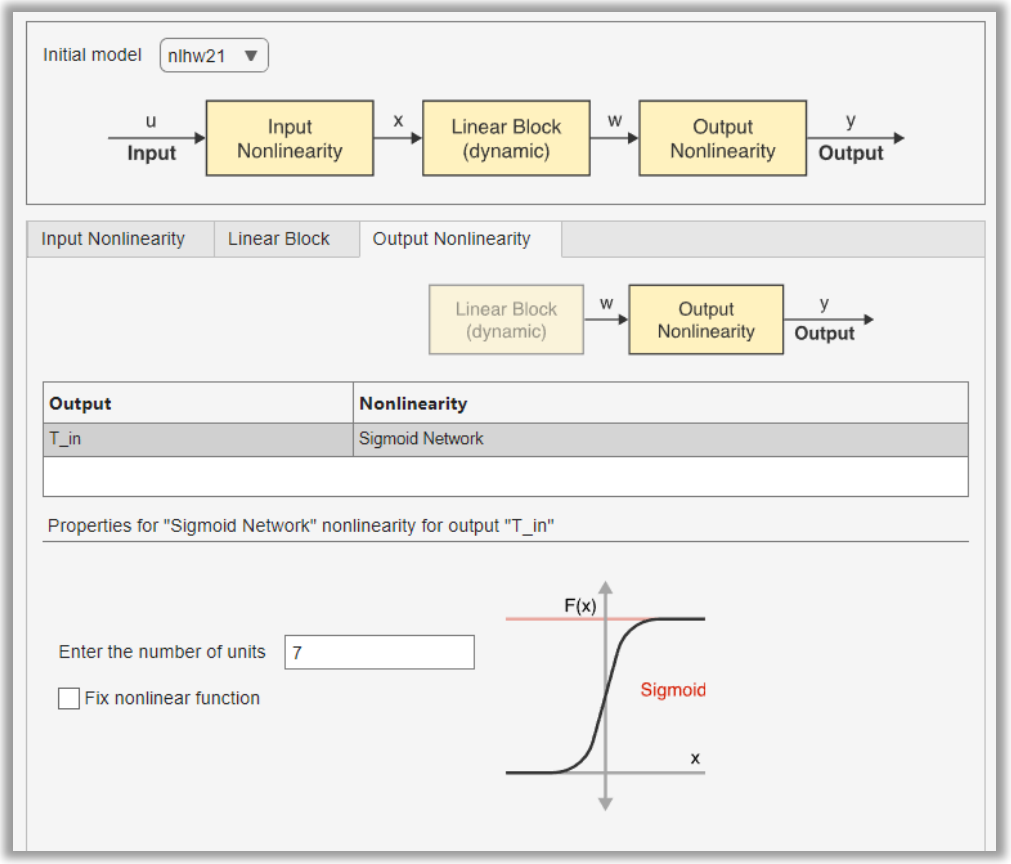

Figure 25. Example: $nlhw21 \rightarrow Number\ of\ Units = 7$

The best new fit is $nlhw21 = 95,88\%$

Customization 3 (Input: Sigmoid Network, Input Number of Units = ? , Output: Sigmoid Network , Output Number of Units = 10)

Table 11. Customization 3 Results

Name	Number of Units (Input)	Fit(%)
nlhw29	10	Nan
nlhw30	5	<80
nlhw31	1	<90

It is observed that the fit does not meet the desired criteria, so the next customization is pursued.

Customization 4 (Input: Sigmoid Network, Input Number of Units = 10 , Output: Piecewise Linear , Output Number of Breakpoints)

Table 12. Customization 4 Results

Name	Number of Breakpoints (Output)	Fit(%)
nlhw32	10	<90
nlhw33	5	<85
nlhw34	1	<80

It is observed that the fit does not meet the desired criteria, so the next customization is pursued.

Customization 5 (Input: Piecewise Linear, Input Number of Breakpoints = 1 , Output: Piecewise Linear , Output Number of Breakpoints)

Table 13. Customization 5 Results

Name	Number of Breakpoints (Output)	Fit(%)
nlhw35	10	83,80
nlhw36	1	<50
nlhw37	2	<50
nlhw38	3	<50
nlhw39	4	83,26
nlhw40	5	82,79
nlhw41	6	84,17
nlhw42	7	<50
nlhw43	8	84,14
nlhw44	9	<50

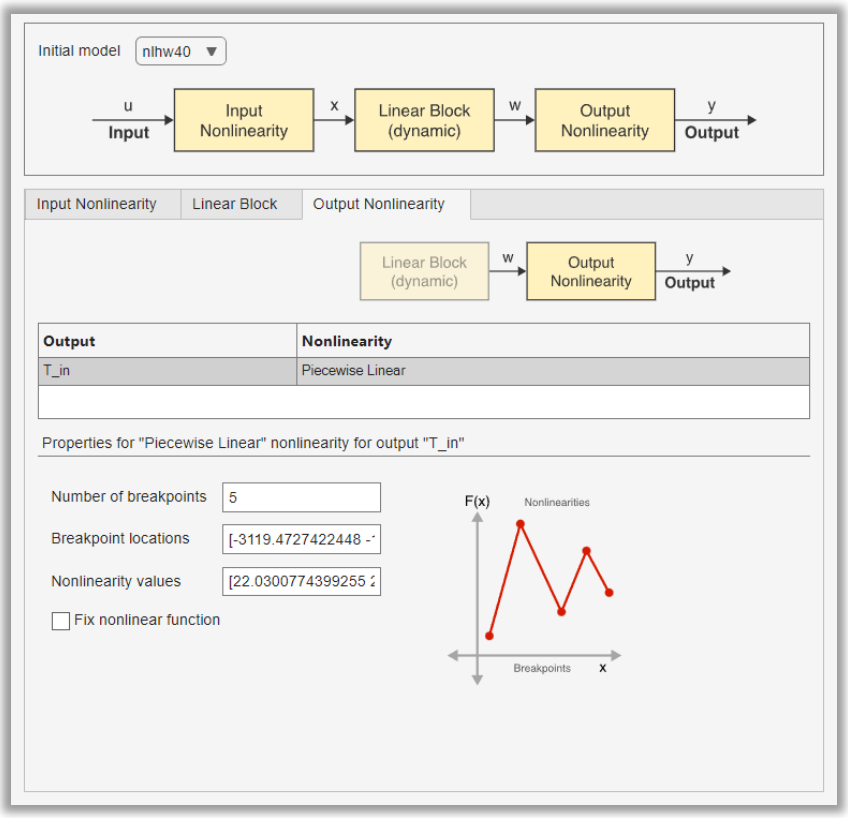

Figure 26. Example: $nlhw40 \rightarrow Number\ of\ breakpoints = 5$

The results of the models extracted for the Hammerstein-Wiener structure for Cluster 1 are as follows. As can be seen from the above, **the model that best fits our system is $\boldsymbol{nlhw21 = 95.88\%}$**. This model corresponds to the following specifications: **Input: Piecewise Linear, Number of breakpoints (Input): 10, Output: Sigmoid Network, and Number of Units (Output): 7**. Similar customizations have been applied to Clusters 2, 3, and 4, and their results are presented below.

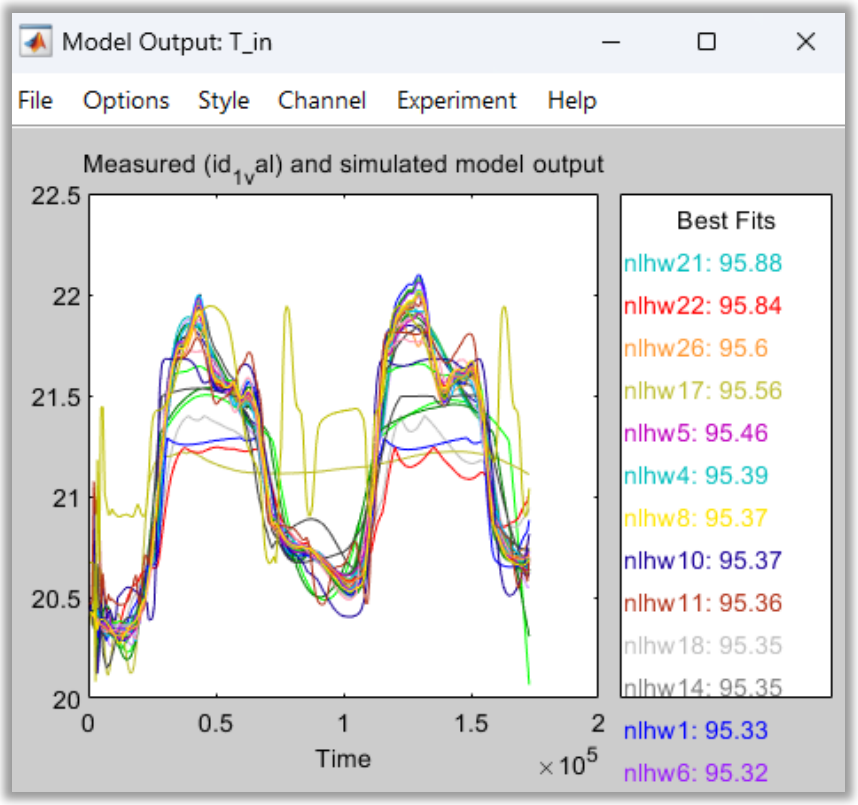

Figure 27. Results of the models extracted for the Hammerstein-Wiener structure for Cluster 1

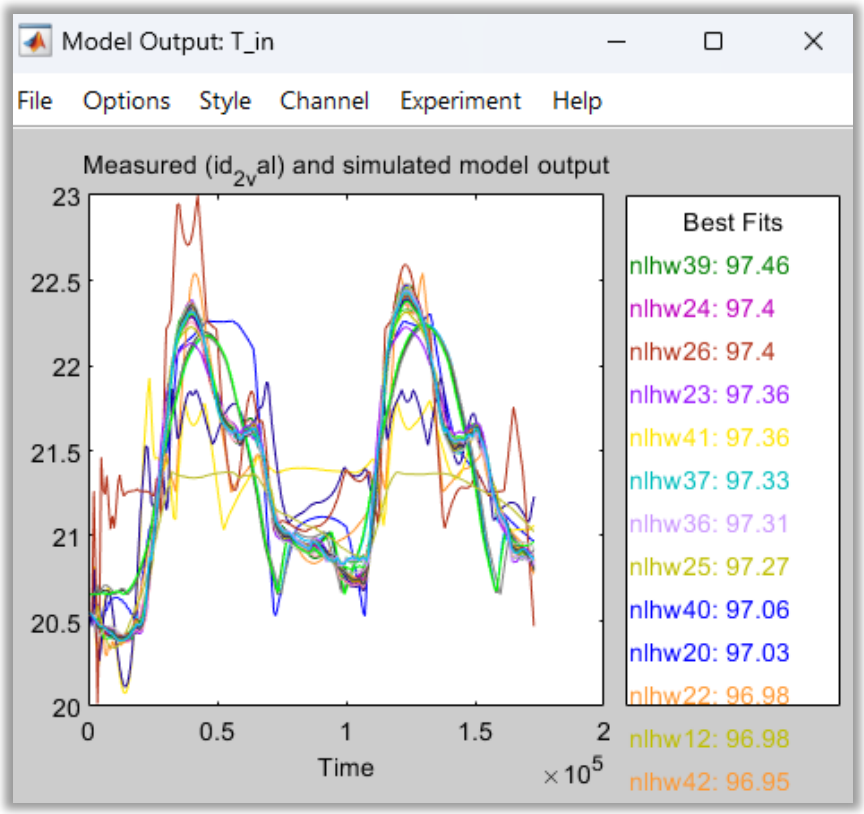

Figure 28. Results of the models extracted for the Hammerstein-Wiener structure for Cluster 2

As observed from the above, **the model that best fits our system is $nlhw39 = 97.46\%$**. This model corresponds to the following specifications: **Input: Sigmoid Network, Number of Units (Input): 3, Output: Piecewise Linear, and Number of breakpoints (Output): 20**.

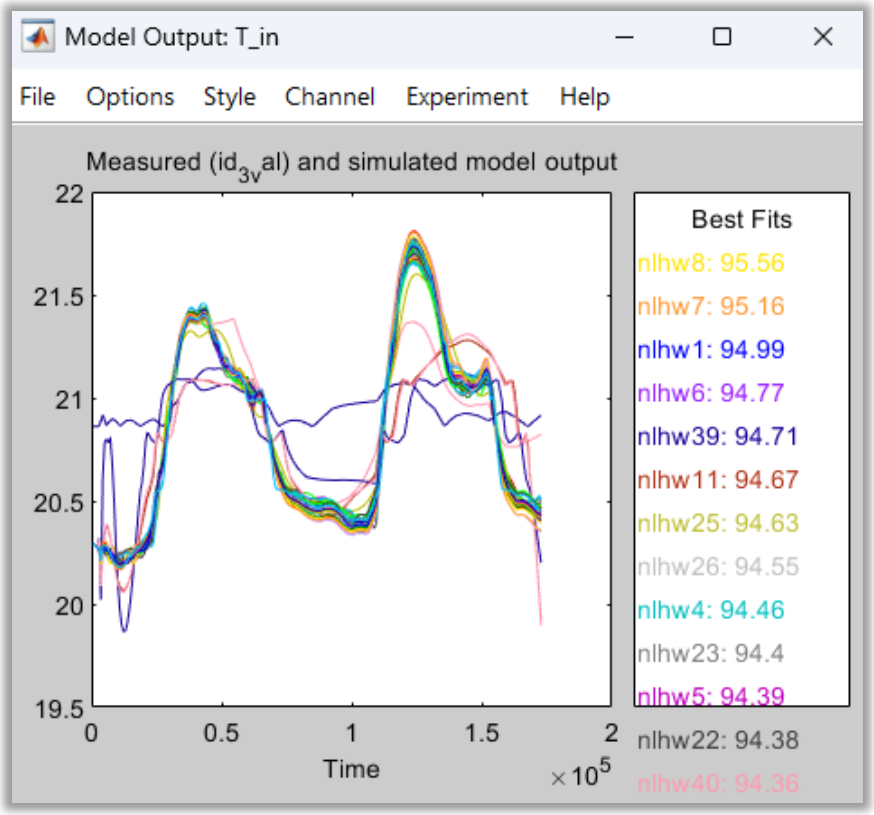

Figure 29. Results of the models extracted for the Hammerstein-Wiener structure for Cluster 3

As observed from the above, **the model that best fits our system is $nlhw8 = 95.56\%$**. This model corresponds to the following specifications: **Input: Piecewise Linear, Number of breakpoints (Input): 7, Output: Piecewise Linear, and Number of breakpoints (Output): 10**.

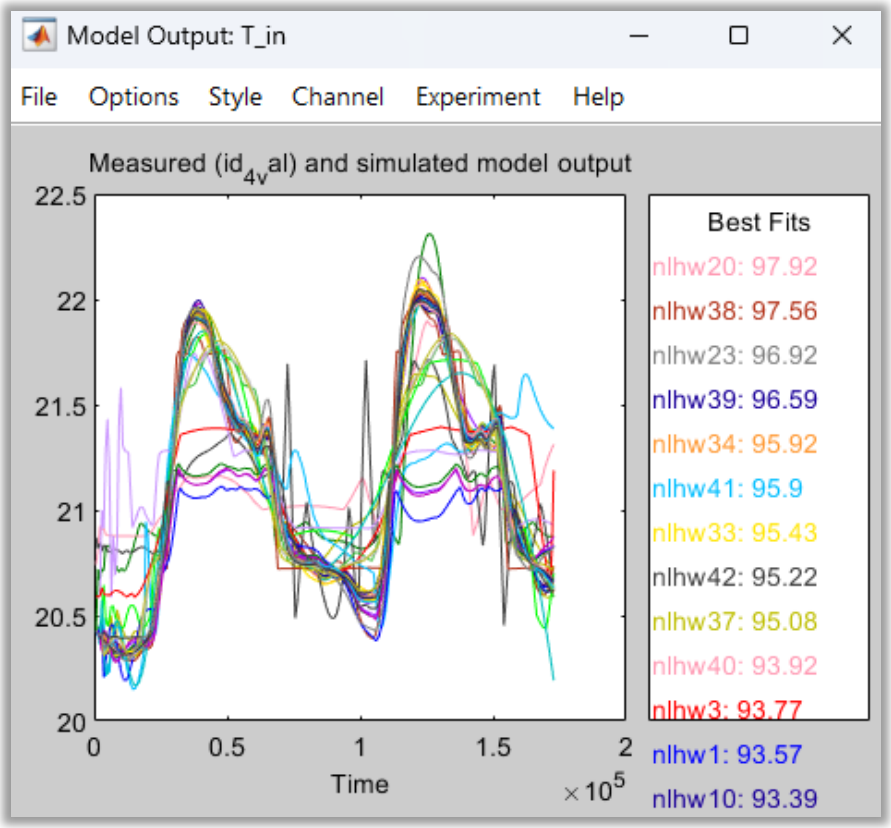

Figure 30. Results of the models extracted for the Hammerstein-Wiener structure for Cluster 4

As observed from the above, **the model that best fits our system is $nlhw20 = 97.92\%$**. This model corresponds to the following specifications: **Input_1: Sigmoid Network, Input_2_3_4: Piecewise Linear, Number of Units (Input_1): 10, Number of breakpoints (Input_2_3_4): 10, Output: Piecewise Linear, and Number of breakpoints (Output): 10**.

5.3.3 Neural Networks

The Neural Network Time Series Toolbox is used to identify a model that fits our system. First, the network to be used is selected from three available choices.

1. **NARX**: In this type of time series problem, we want to predict future values of series $y(t)$ from past values of that time series and past values of a second time series $x(t)$.
2. **NAR**: In this type of time series problem, we want to predict future values of series $y(t)$ from past values of that series only.
3. **Nonlinear Input-Output Network**: In this type of time series problem, we have an input series $x(t)$ and an output series $y(t)$. We want to predict future values of $y(t)$ from previous values of $x(t)$.

In this case, the NARX network is selected because the prediction of future values of the output T_{in} ($y(t)$) from past values of all inputs $x(t)$ and past values of the output $y(t)$ is desired.

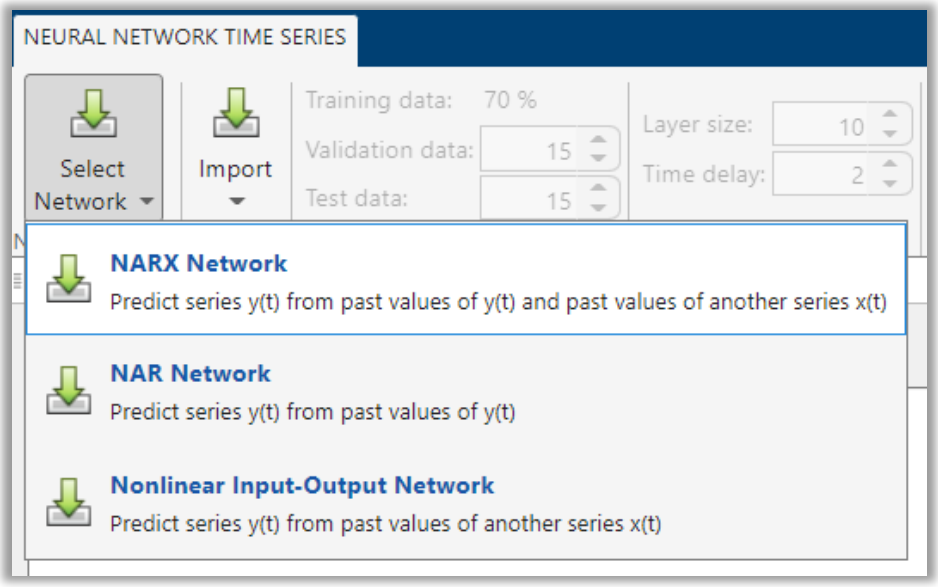

Figure 31. Network Selection

The data for each cluster is selected and imported, as shown below. For Cluster 1, the data consists of:

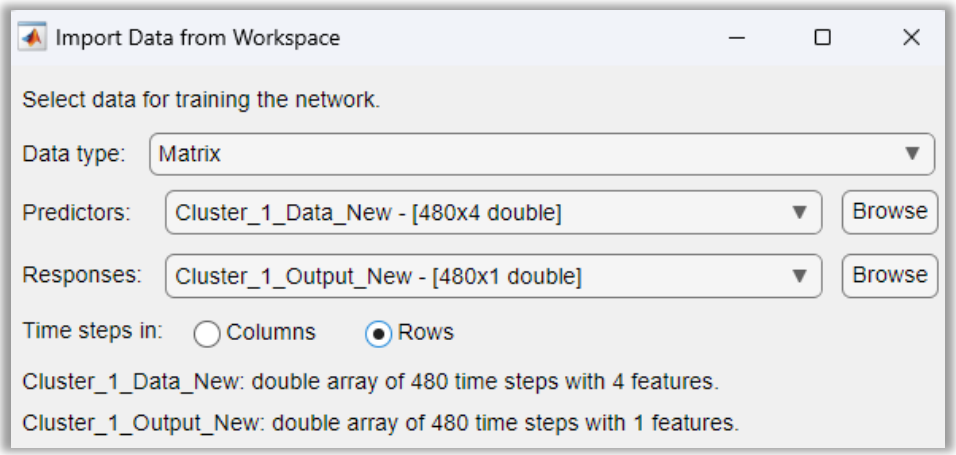

Figure 32. Import data for cluster 1

For each cluster, the same Training data, Validation data, Test data, Layer Size, and Time delay are chosen.

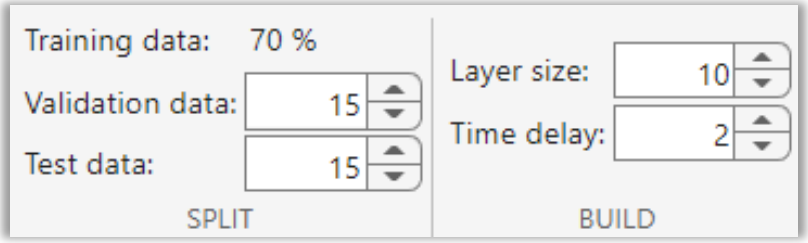

Figure 33. Import data for cluster 1

The Neural Network is trained, and the results for all clusters are presented below.

The MSE variable represents the mean squared error between outputs and responses, while the R variable denotes the correlation between outputs and responses.

Cluster 1

Training Results

Training finished: Met validation criterion

Training Progress

Unit	Initial Value	Stopped Value	Target Value
Epoch	0	36	1000
Elapsed Time	-	00:00:00	-
Performance	4.69	1.06e-05	0
Gradient	9.43	0.000262	1e-07
Mu	0.001	1e-06	1e+10
Validation Checks	0	6	6

Figure 34: Training Progress for Cluster 1

Algorithm

Data division: Random
Training algorithm: Levenberg-Marquardt
Performance: Mean squared error

Training Results

Training start time: 22-Jul-2024 13:33:59
Layer size: 10
Time delay: 2

	Observations	MSE	R
Training	334	1.0981e-05	1.0000
Validation	72	9.9277e-06	1.0000
Test	72	1.7817e-05	1.0000

Figure 35: Training Results for Cluster 1

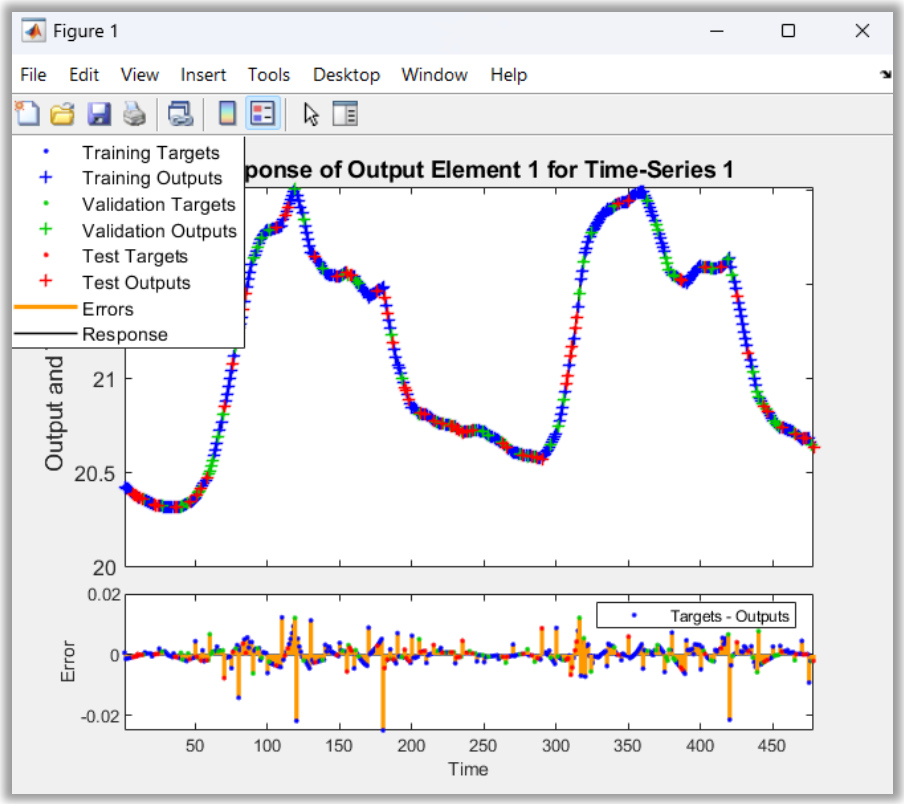

Figure 36. Results of the models extracted for Neural Networks structure for Cluster 1

Cluster 2

Training Results

Training finished: Met validation criterion

Training Progress

Unit	Initial Value	Stopped Value	Target Value
Epoch	0	46	1000
Elapsed Time	-	00:00:00	-
Performance	1.81	8.47e-06	0
Gradient	5.92	0.000465	1e-07
Mu	0.001	1e-06	1e+10
Validation Checks	0	6	6

Figure 37: Training Progress for Cluster 2

Algorithm

Data division: Random
Training algorithm: Levenberg-Marquardt
Performance: Mean squared error

Training Results

Training start time: 22-Jul-2024 13:43:43
Layer size: 10
Time delay: 2

	Observations	MSE	R
Training	334	8.8507e-06	1.0000
Validation	72	1.6341e-05	1.0000
Test	72	1.1041e-05	1.0000

Figure 38: Training Results for Cluster 2

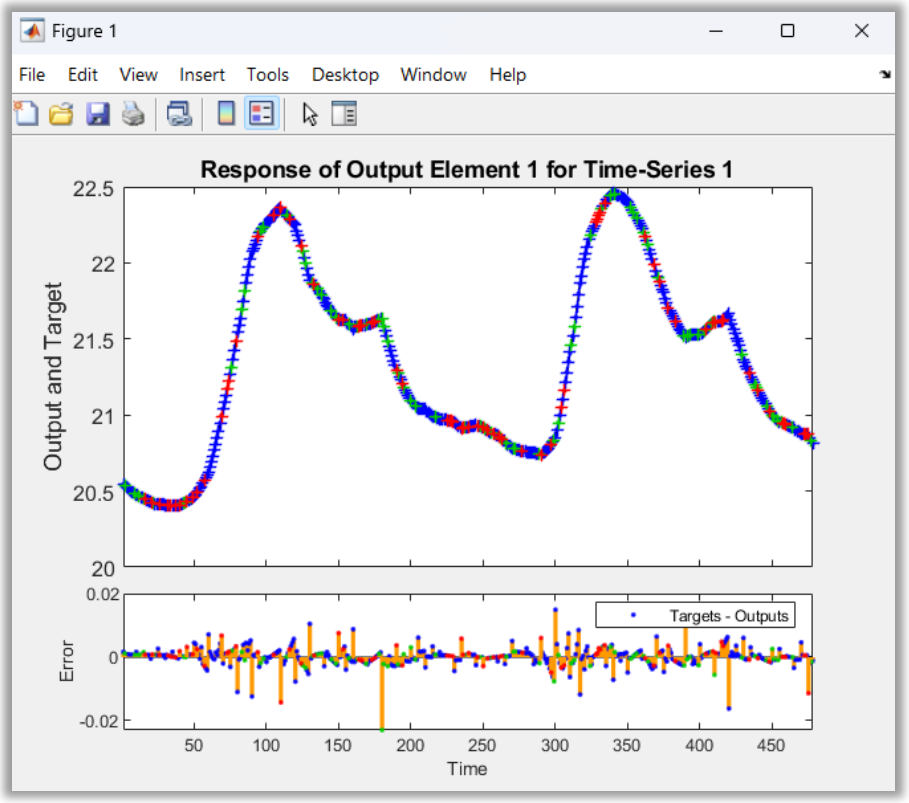

Figure 39. Results of the models extracted for Neural Networks structure for Cluster 2

Cluster 3

Training Results

Training finished: Met validation criterion

Training Progress

Unit	Initial Value	Stopped Value	Target Value
Epoch	0	17	1000
Elapsed Time	-	00:00:00	-
Performance	7.12	6.81e-06	0
Gradient	11.2	4.86e-05	1e-07
Mu	0.001	1e-06	1e+10
Validation Checks	0	6	6

Figure 40: Training Progress for Cluster 3

Algorithm

Data division: Random
Training algorithm: Levenberg-Marquardt
Performance: Mean squared error

Training Results

Training start time: 22-Jul-2024 13:56:37
Layer size: 10
Time delay: 2

	Observations	MSE	R
Training	334	6.9320e-06	1.0000
Validation	72	7.8531e-06	1.0000
Test	72	9.8895e-06	1.0000

Figure 41: Training Results for Cluster 3

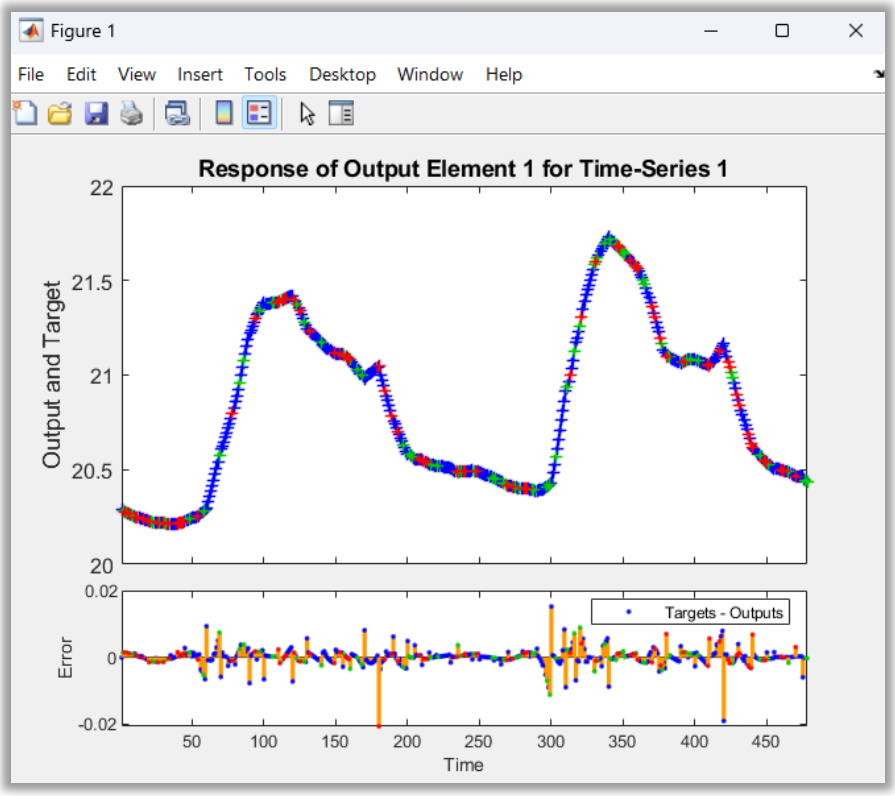

Figure 42. Results of the models extracted for Neural Networks structure for Cluster 3

Cluster 4

Training Results

Training finished: Met validation criterion

Training Progress

Unit	Initial Value	Stopped Value	Target Value
Epoch	0	167	1000
Elapsed Time	-	00:00:00	-
Performance	1.18	5.62e-06	0
Gradient	4.55	6.6e-05	1e-07
Mu	0.001	1e-06	1e+10
Validation Checks	0	6	6

Figure 43: Training Progress for Cluster 4

Algorithm

Data division: Random
Training algorithm: Levenberg-Marquardt
Performance: Mean squared error

Training Results

Training start time: 22-Jul-2024 14:00:15
Layer size: 10
Time delay: 2

	Observations	MSE	R
Training	334	5.6657e-06	1.0000
Validation	72	1.8643e-05	1.0000
Test	72	7.3105e-06	1.0000

Figure 44: Training Results for Cluster 4

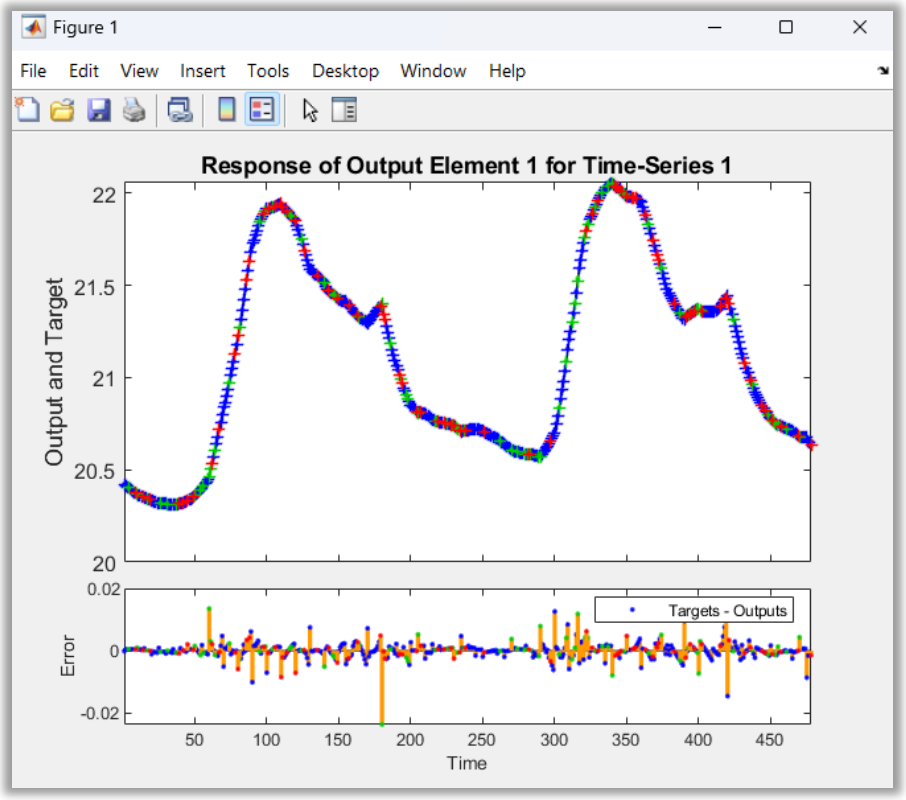

Figure 45. Results of the models extracted for Neural Networks structure for Cluster 4

Chapter 6

Parameter Estimation in Building Energy Management and Control

6.1 Parameter Estimation

Parameter estimation techniques are crucial for building energy management and control, significantly contributing to the efficiency, reliability, and optimization of energy usage. Accurate parameter estimation forms the foundation for reliable energy models, enhancing predictive accuracy and enabling better planning and resource allocation. It allows for the fine-tuning of HVAC systems, lighting, and other energy-consuming equipment, leading to more efficient operation and reduced energy waste. Dynamic and adaptive control strategies, informed by real-time parameter estimation, can adjust settings to maintain comfort and efficiency based on current conditions. This leads to lower energy bills, reduced operational costs, and justified investments in energy-saving technologies. Furthermore, accurate parameter estimation ensures occupant comfort and productivity by maintaining optimal indoor environments, thus enhancing health and well-being. It also supports sustainability goals by reducing the carbon footprint and ensuring compliance with energy efficiency standards.

6.2 Problem Formulation

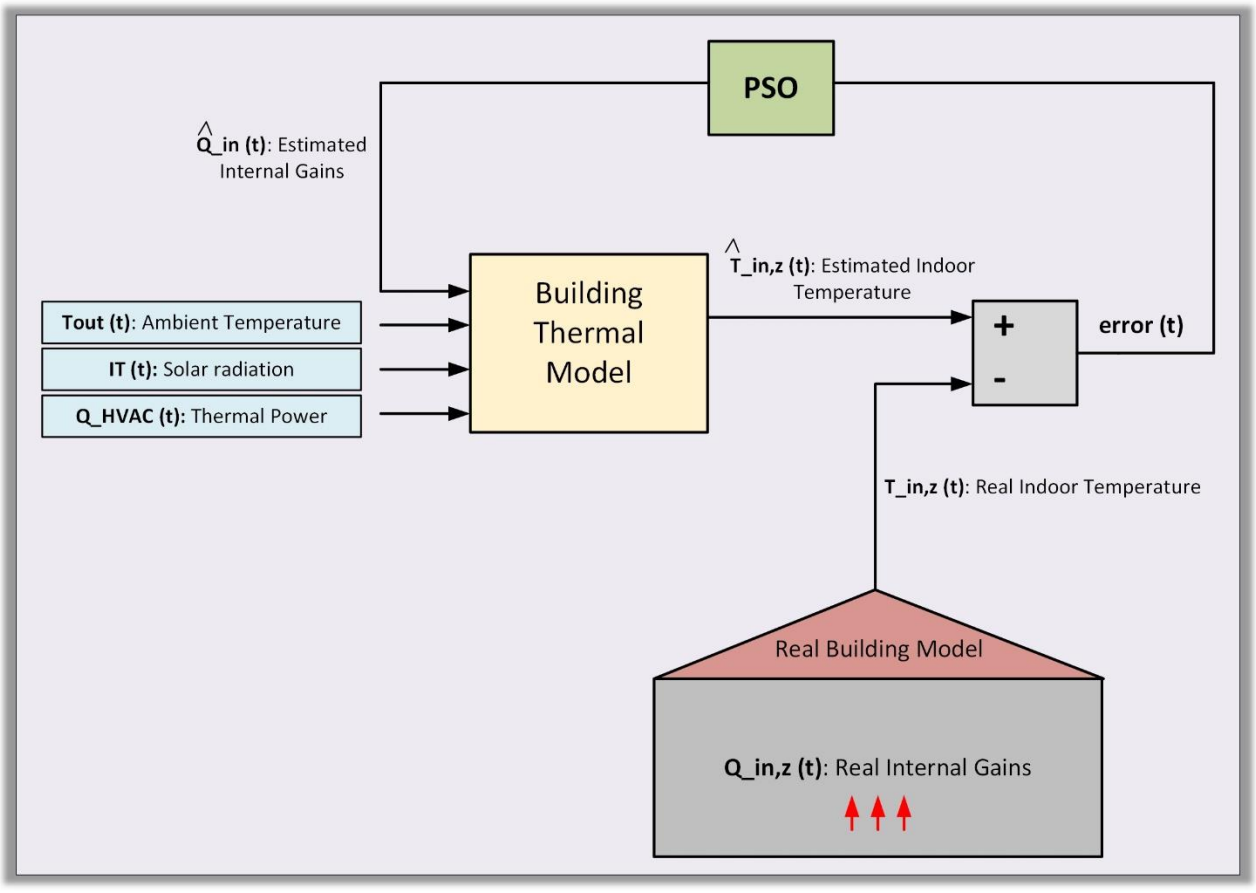

Figure 46. Structure of the examined problem

In the context of real-time building energy management and control, **accurate estimation of internal thermal gains** is critical for maintaining indoor comfort and optimizing energy usage. This problem involves utilizing a building thermal model to estimate internal thermal gains of each building thermal zone and comparing these estimations with real measurements from a building. The PSO algorithm is employed to minimize the error between estimated and actual indoor temperatures.

Measurement and Data Collection

Real-time measurements from a building include the following parameters:

- Internal thermal gains of each thermal zone $Q_{in,z}$
- Thermal power consumption of the HVAC system for each thermal zone $Q_{HVAC,z}$
- Indoor temperature of each thermal zone $T_{in,z}$
- Ambient temperature T_{out}
- Solar radiation I_T

These real measurements are used as inputs and comparison benchmarks in the building thermal model.

Building Thermal Model

A building thermal model is employed to estimate internal thermal gains. The inputs to this model are:

- Ambient temperature T_{out}
- Solar radiation I_T
- HVAC thermal power consumption of each thermal zone $Q_{HVAC,z}$
- Estimated internal thermal gains of each thermal zone (decision variable for PSO) $Q_{in,z,est}$

The model predicts the indoor temperature of each thermal zone, $T_{in,z,est}$, based on these inputs.

Objective Function and Optimization

The PSO algorithm is used to find the optimal values of the estimated internal thermal gains of each building thermal zone. The objective function for the PSO is defined as the sum of the errors between the estimated indoor temperatures and the actual indoor temperatures for each thermal zone, as given in (34). The steps involved are:

1. **Estimation**: The building thermal model estimates the indoor temperature for each thermal zone using the given inputs.
2. **Comparison**: The estimated indoor temperatures are compared with the actual indoor temperatures measured in the building.
3. **Error Calculation**: The error for each thermal zone is calculated as the difference between the estimated and actual indoor temperatures.
4. **Summation**: The errors from all thermal zones are summed to form the objective function.
5. **Optimization**: The PSO algorithm iteratively adjusts the estimated internal thermal gains to minimize the objective function, thereby reducing the overall error and aligning the estimated indoor temperatures with the actual measurements.

$$\boldsymbol{objective\_function} = \min_{\boldsymbol{Q_{in,z,est}}} \sum_{\boldsymbol{z=1}}^{\boldsymbol{N_z}} \left(\boldsymbol{T_{in,z,est}(t)} - \boldsymbol{T_{in,z}(t)}\right)^2 \quad (34)$$

Methodology

1. **Data Acquisition**: Real-time data for ambient temperature, solar radiation, HVAC power consumption, and indoor temperatures are collected.
2. **Model Input**: These measurements are input into the building thermal model along with initial estimates of internal thermal gains.
3. **Simulation**: The model simulates indoor temperatures for each thermal zone.
4. **Error Computation**: The difference between the simulated indoor temperatures and the actual measurements is computed.
5. **PSO Implementation**: PSO is applied to iteratively adjust the internal thermal gains. Each particle in the swarm represents a potential solution, and the algorithm seeks to minimize the objective function.
6. **Optimization Process**: Through iterations, the PSO algorithm finds the optimal set of internal thermal gains that minimize the error, ensuring the estimated indoor temperatures are as close as possible to the actual measurements.

6.3 Results

The floor plan of **11 building thermal zones** is given in Figure 7. Table 1 and Figure 8 provide the data were used. Figures (48)-(58) present the actual internal thermal gains together with the estimated internal thermal gains for each building thermal zone. It follows that the proposed parameter estimation technique provides high performance, as the estimation of the internal thermal gains of the building thermal zones is successful since it is very well aligned with the actual data.

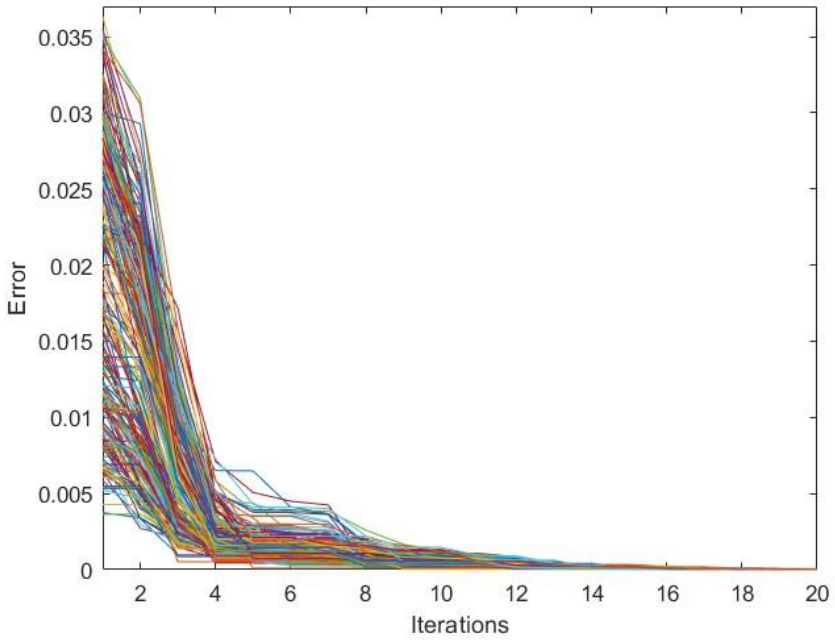

Figure 56. Evolution of the error over the iterations of PSO

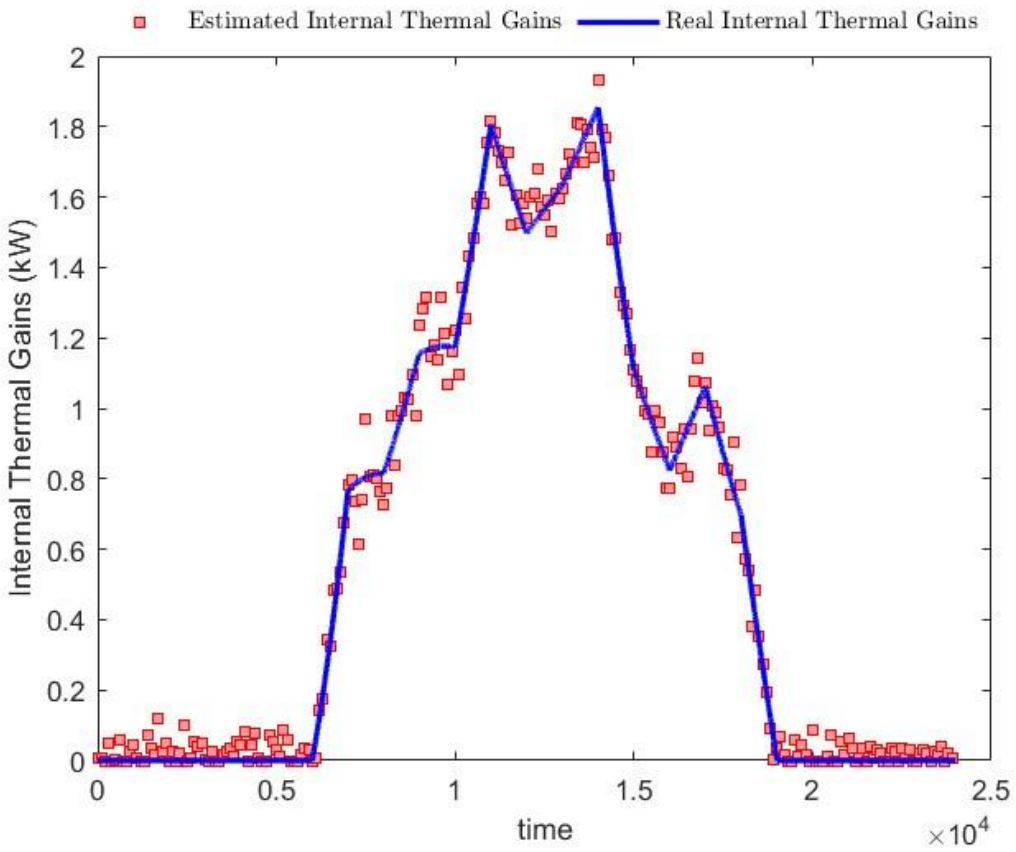

Figure 48. Actual and estimated internal thermal gains – Thermal zone 1

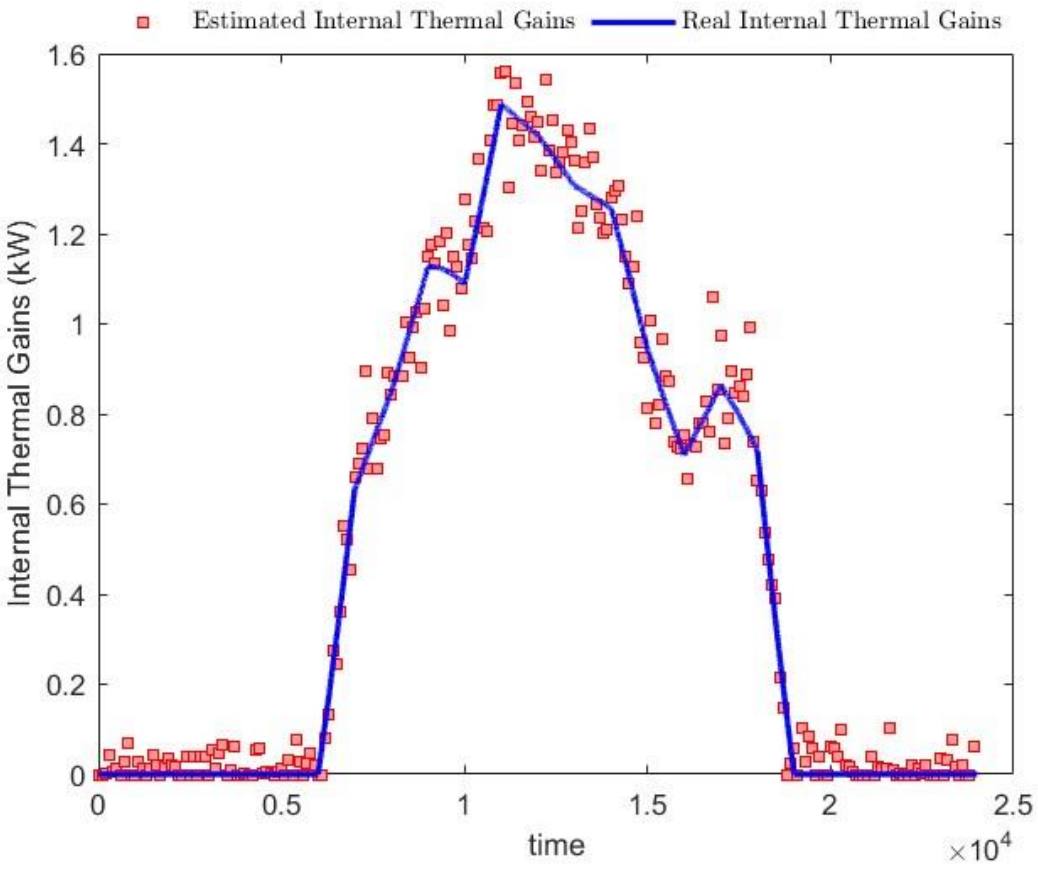

Figure 49. Actual and estimated internal thermal gains – Thermal zone 2

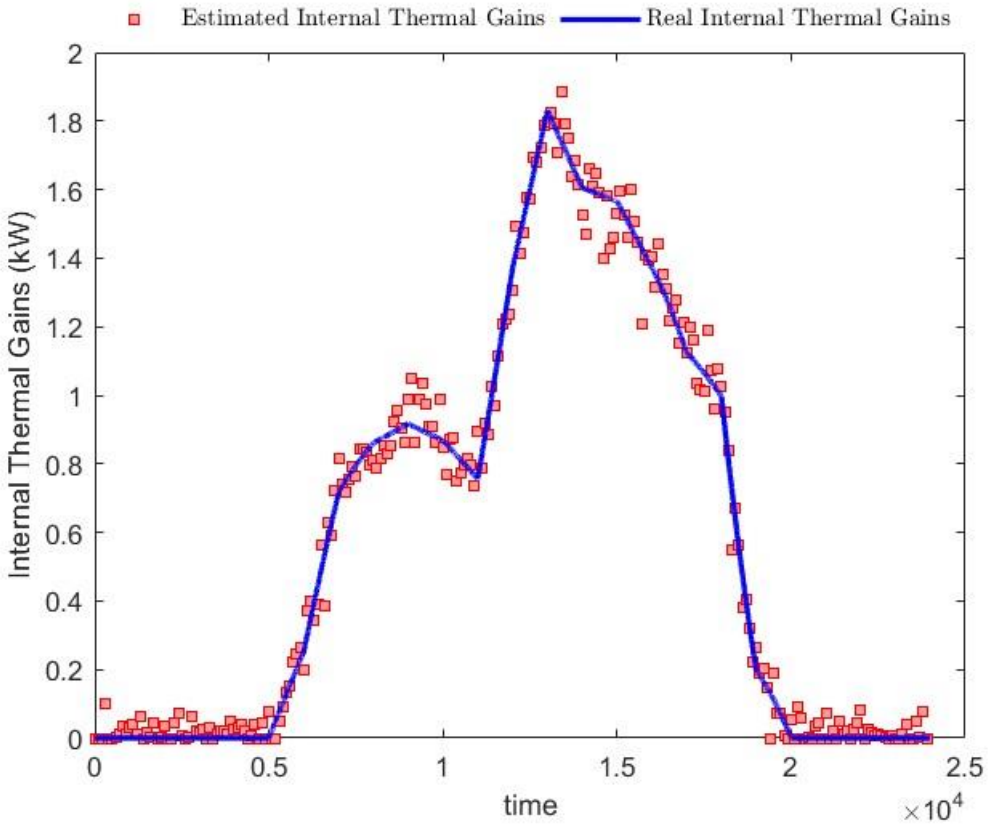

Figure 50. Actual and estimated internal thermal gains – Thermal zone 3

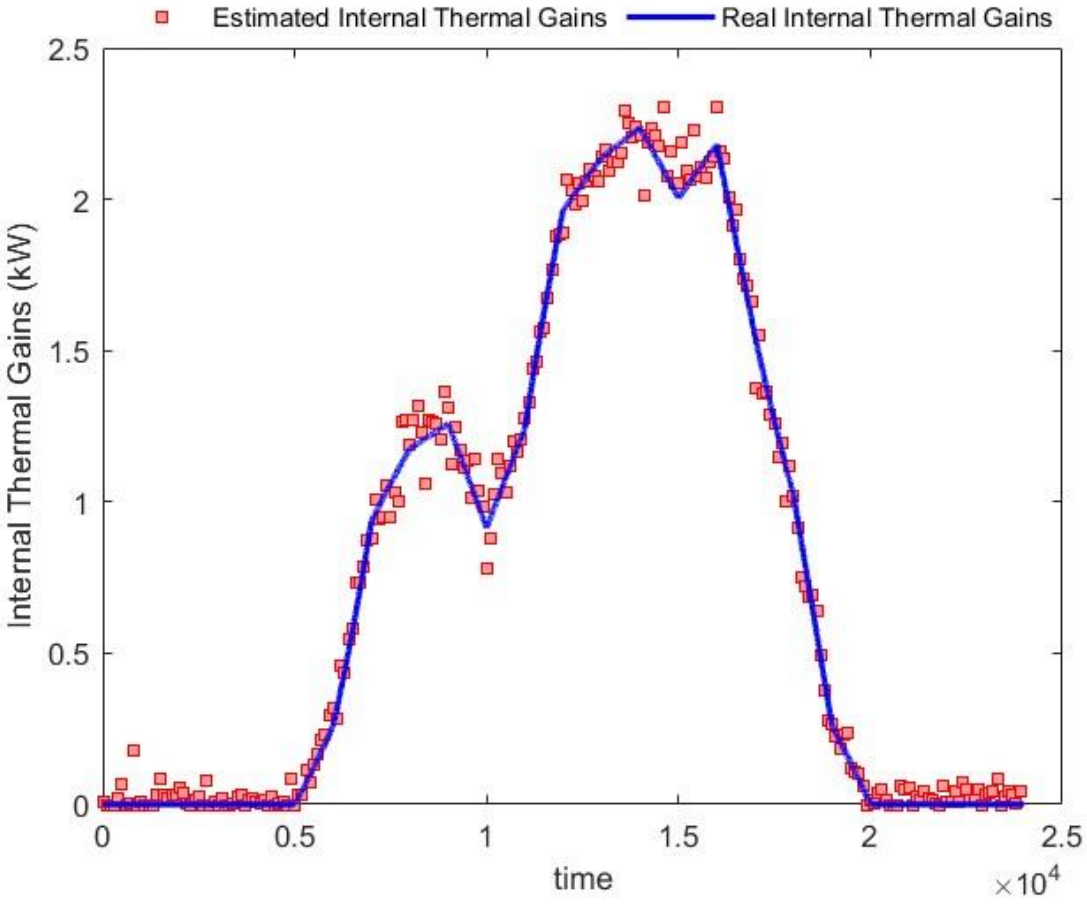

Figure 51. Actual and estimated internal thermal gains – Thermal zone 4

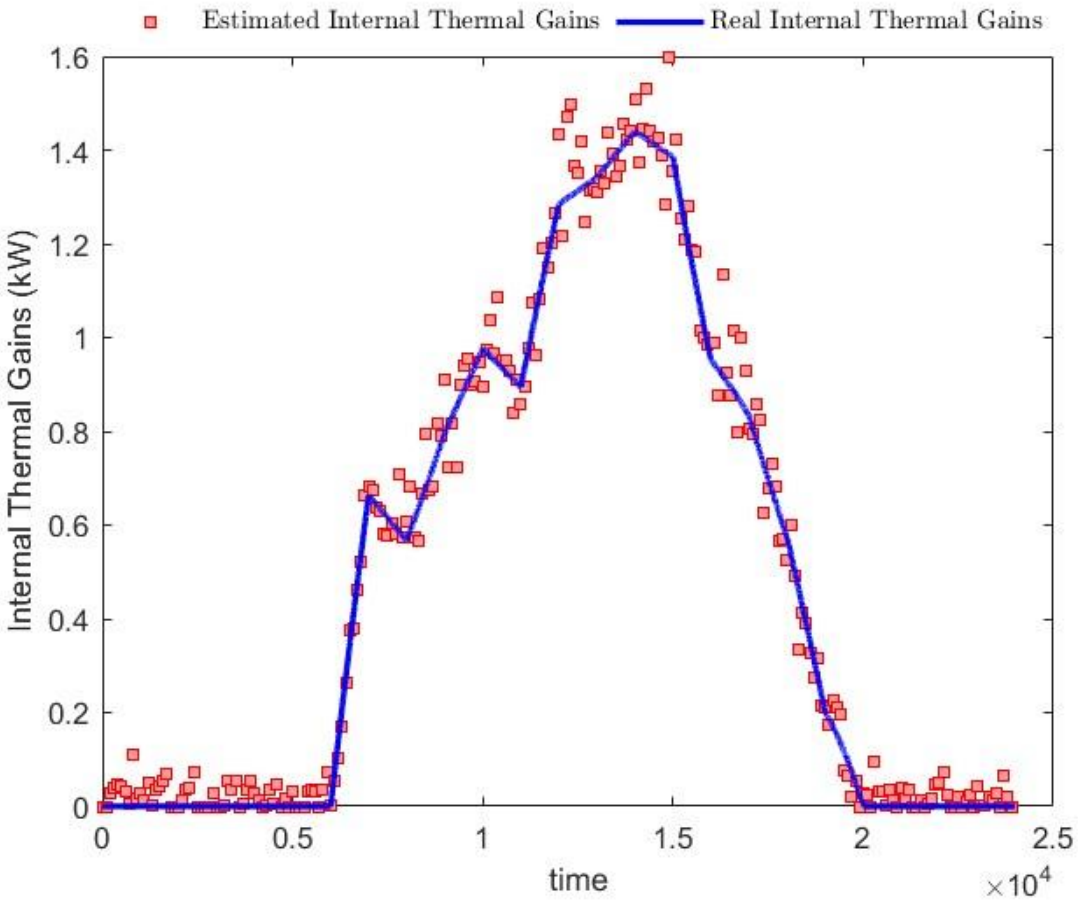

Figure 52. Actual and estimated internal thermal gains – Thermal zone 5

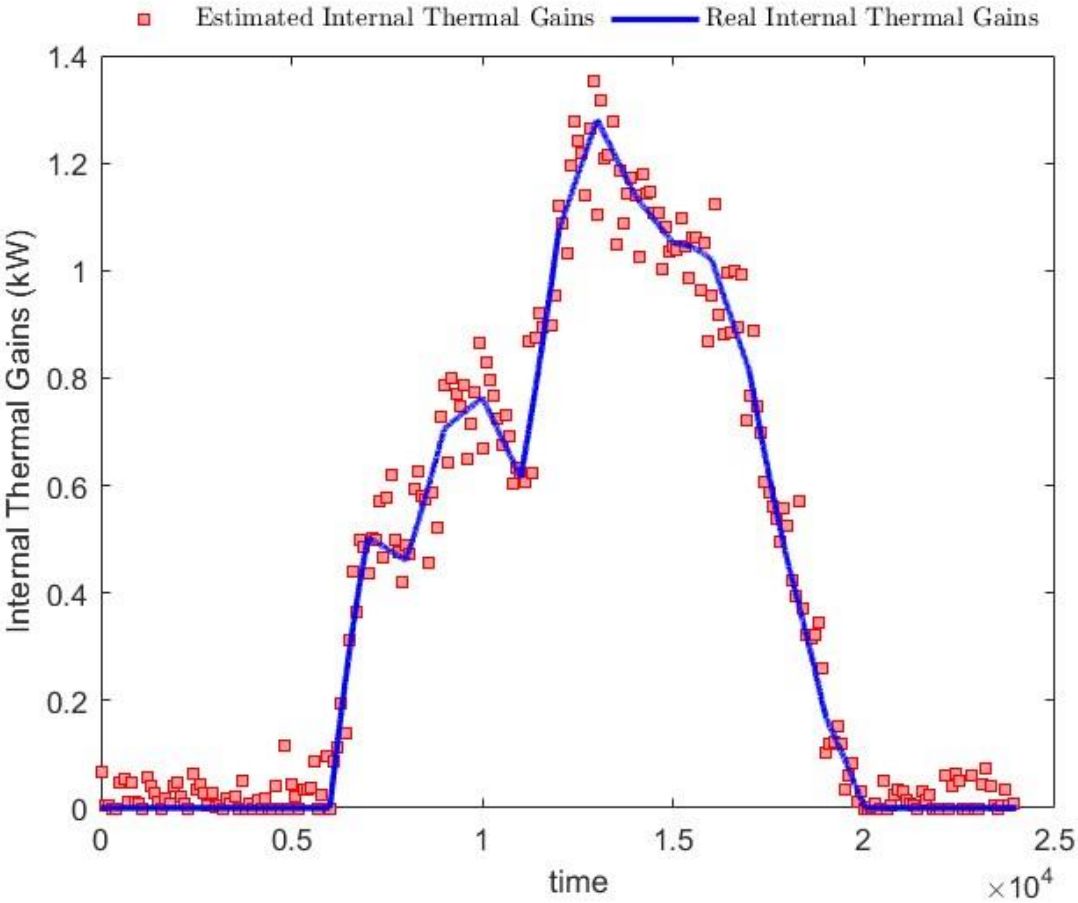

Figure 53. Actual and estimated internal thermal gains – Thermal zone 6

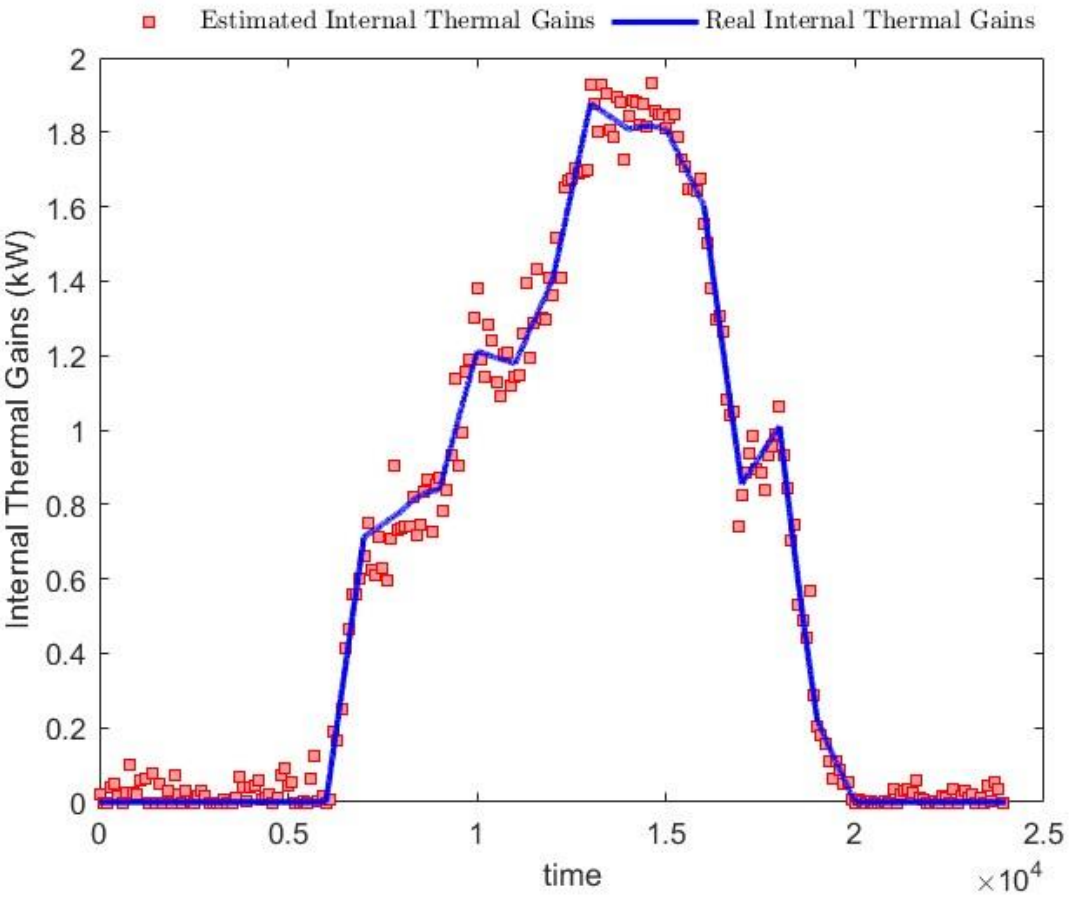

Figure 54. Actual and estimated internal thermal gains – Thermal zone 7

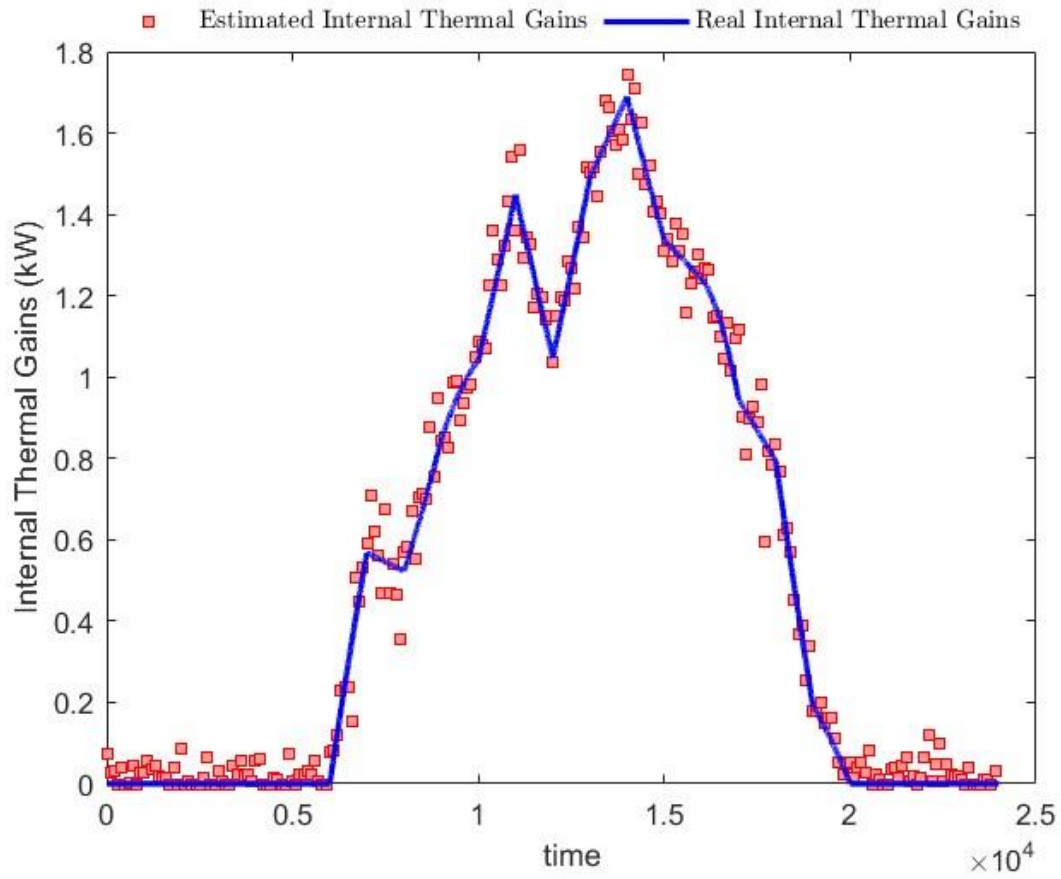

Figure 55. Actual and estimated internal thermal gains – Thermal zone 8

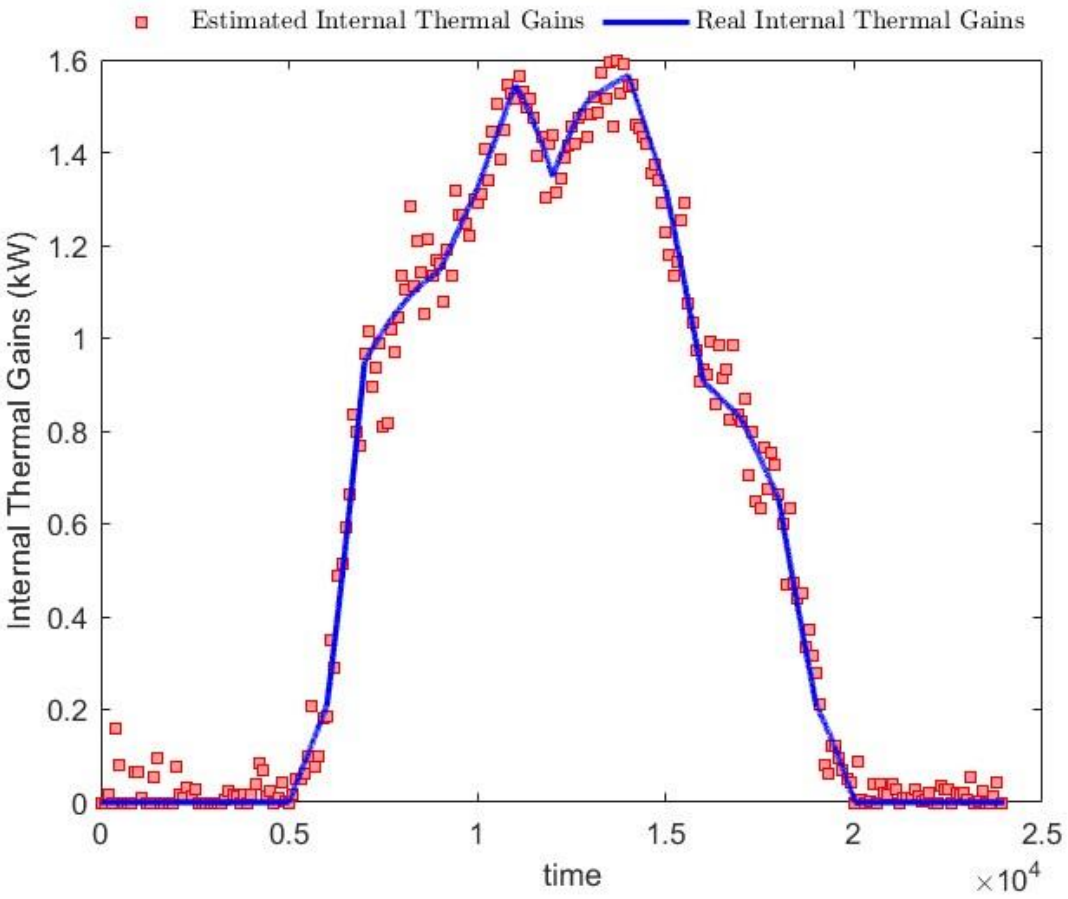

Figure 56. Actual and estimated internal thermal gains – Thermal zone 9

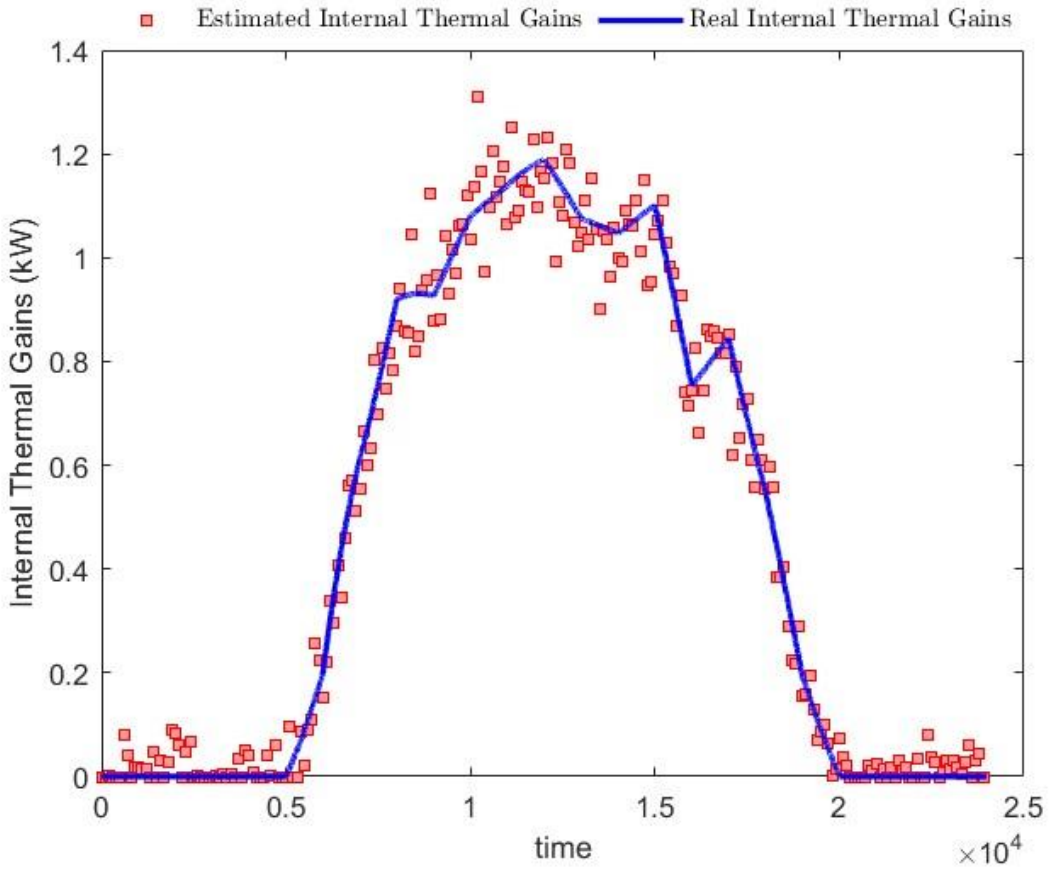

Figure 57. Actual and estimated internal thermal gains – Thermal zone 10

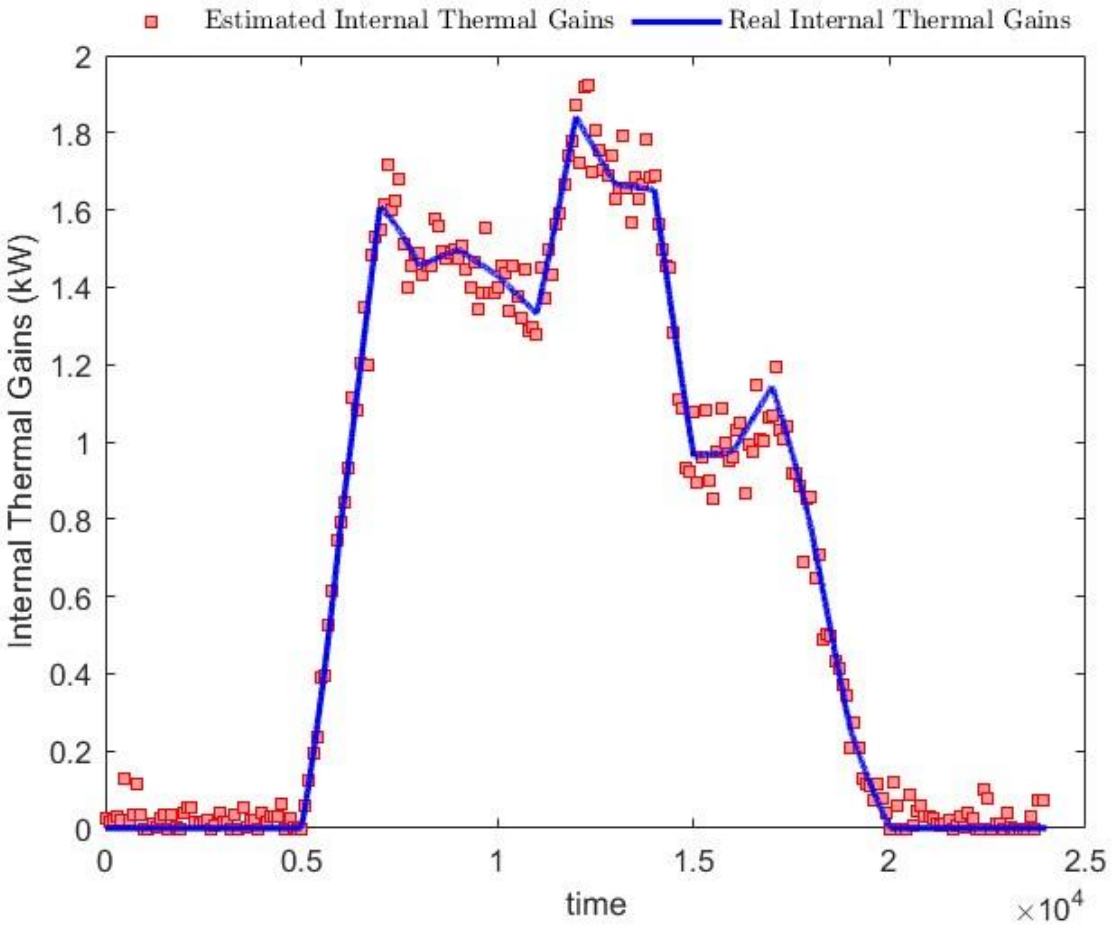

Figure 58. Actual and estimated internal thermal gains – Thermal zone 11

Chapter 7

Conclusion

In this work, system identification and parameter estimation techniques are used. An accurate model for estimating the indoor temperature of building thermal zones was developed, which is crucial for energy management and occupant comfort. Four key inputs were incorporated into the model: internal thermal loads from occupants, lighting, and equipment; the HVAC system's power consumption; ambient temperature; and solar irradiation. Advanced modeling techniques, such as system identification and neural networks, were applied to capture the dynamic behavior and complex, nonlinear relationships influencing indoor temperature.

Moreover, this work presents a sophisticated approach to real-time building energy management through the accurate estimation of internal thermal gains. By leveraging a building thermal model and employing Particle Swarm Optimization (PSO), the discrepancies between estimated and actual indoor temperatures are minimized, leading to optimized HVAC performance and enhanced occupant comfort. The methodology demonstrates the effectiveness of using real-time data inputs, such as ambient temperature, solar radiation, and HVAC power consumption, to refine model predictions and ensure energy-efficient building operations. The integration of PSO in this context underscores its potential in solving complex optimization challenges within building energy management.

In conclusion, the developed tools can be very useful in energy management and real-time control applications of building energy systems. The detailed model of the building energy system developed is the basis on which the applied identification techniques are based, as well as any real-time control system of the building energy system.

References

[1] https://ec.europa.eu/energy/en/topics/energy-efficiency/buildings

[2] "Transition to Sustainable Buildings", Strategies and Opportunities to 2050, IEA, 2013.

[3] Thomas, D.; Deblecker, O.; Ioakimidis, C.S. Optimal operation of an energy management system for a grid-connected smart building considering photovoltaics' uncertainty and stochastic electric vehicles' driving schedule. Appl. Energy 2018, 210, 1188–1206.

[4] Sturzenegger, D.; Gyalistras, D.; Morari, M.; Smith, R.S. Model Predictive Climate Control of a Swiss Office Building: Implementation, Results, and Cost-Benefit Analysis. IEEE Trans. Control. Syst. Technol. 2016, 24, 1–12.

[5] Carli, R.; Dotoli, M. Decentralized control for residential energy management of a smart users' microgrid with renewable energy exchange. IEEE/CAA J. Autom. Sin. 2019, 6, 641–656.

[6] Alibabaei, N.; Fung, A.S.; Raahemifar, K.; Moghimi, A. Effects of intelligent strategy planning models on residential HVAC system energy demand and cost during the heating and cooling seasons. Appl. Energy 2017, 185, 29–43.

[7] Akter, M.N.; Mahmud, M.A.; Oo, A.M.T. A hierarchical transactive energy management system for energy sharing in residential microgrids. Energies 2017, 10, 12.

[8] Jiang, Q.; Xue, M.; Geng, G. Energy management of microgrid in grid-connected and stand-alone modes. IEEE Trans. Power Syst. 2013, 28, 3380–3389.

[9] Li, Z.; Xu, Y. Optimal coordinated energy dispatch of a multi-energy microgrid in grid-connected and islanded modes. Appl. Energy 2018, 210, 974–986.

[10] Worku, M.Y.; Hassan, M.A.; Abido, M.A. Real time energy management and control of renewable energy based microgrid in grid connected and Island modes. Energies 2019, 12, 276.

[11] Zheng, Y.; Li, S.; Tan, R. Distributed Model Predictive Control for On-Connected Microgrid Power Management. IEEE Trans. Control. Syst. Technol. 2018, 26, 1028–1039.

[12] Zhang, Y.; Gatsis, N.; Giannakis, G.B. Robust energy management for microgrids with high-penetration renewables. IEEE Trans. Sustain. Energy 2013, 4, 944–953.

[13] Pinzon, J.A.; Vergara, P.P.; Da Silva, L.C.P.; Rider, M.J. Optimal Management of Energy Consumption and Comfort for Smart Buildings Operating in a Microgrid. IEEE Trans. Smart Grid 2019, 10, 3236–3247.

[14] Pinzon, J.A.; Vergara, P.P.; Da Silva, L.C.P.; Rider, M.J. A MILP model for optimal management of energy consumption and comfort in smart buildings. In Proceedings of the 2017 IEEE Power and Energy Society Innovative Smart Grid Technologies Conference, ISGT, Arlington, VA, USA, 2017, 23–26 April 2017.

[15] Hao, H.; Corbin, C.D.; Kalsi, K.; Pratt, R.G. Transactive Control of Commercial Buildings for Demand Response. IEEE Trans. Power Syst. 2017, 32, 774–783.

[16] Bharati, G.R.; Razmara, M.; Paudyal, S.; Shahbakhti, M.; Robinett, R.D. Hierarchical optimization framework for demand dispatch in building-grid systems. In Proceedings of the IEEE Power and Energy Society General Meeting, Boston, MA, USA, 17–21 July 2016.

[17] Tavakoli, M.; Shokridehaki, F.; Marzband, M.; Godina, R.; Pouresmaeil, E. A two-stage hierarchical control approach for the optimal energy management in commercial building microgrids based on local wind power and PEVs. Sustain. Cities Soc. 2018, 41, 332–340.

[18] Jin X., Wu J., Mu Y., Wang M., Xu X. & Jia H., "Hierarchical microgrid energy management in an office building", Applied Energy, vol. 208, pp. 480-494, 2017.

[19] Kyriakou D.G., Kanellos F.D., "Optimal Operation of Microgrids Comprising Large Building Prosumers and Plug-in Electric Vehicles Integrated into Active Distribution Networks," Energies, vol. 15, no. 17, pp. 6182, 2022.

[20] Farinis G.K., Kanellos F.D., "Integrated energy management system for Microgrids of building prosumers", Electric Power Systems Research, vol. 198, 2021.

[21] Kyriakou D.G., Kanellos F.D., "Sustainable Operation of Active Distribution Networks", Applied Sciences, vol.13, no. 5, p. 3115, Feb. 2023.

[22] Kyriakou D.G., Kanellos F.D., "Energy and power management system for microgrids of large-scale building prosumers", IET Energy Syst. Integr. 1– 17 (2023).

[23] Kyriakou D.G., Kanellos F.D., "Optimal Frequency Support Method for Urban Microgrids of Building Prosumers", Sustainable Cities and Society, vol. 98, 104776, 2023.

[24] Kyriakou D.G., Kanellos F.D., Ipsakis D., "Multi-agent-based real-time operation of microgrids employing plug-in electric vehicles and building prosumers", Sustainable Energy, Grids and Networks, vol. 37, 101229, 2024.

[25]https://www.mathworks.com/videos/system-identification-part-1-what-is-system-identification-1636628273301.html

[26]https://www.mathworks.com/videos/system-identification-part-2-linear-system-identification-1636629439565.html

[27]https://www.mathworks.com/videos/system-identification-part-3-nonlinear-system-identification-1641278166243.html

[28] https://www.mathworks.com/help/ident/gs/about-system-identification.html

[29] https://apmonitor.com/dde/index.php/Main/AutoRegressive

[30] https://www.researchgate.net/figure/The-structure-of-a-nonlinear-ARX-model_fig2_329972298

[31] https://www.mathworks.com/help/ident/ug/what-are-hammerstein-wiener-models.html

[32] https://en.wikipedia.org/wiki/Neural_network_(machine_learning)

[33] https://www.mathworks.com/discovery/neural-network.html

[34] https://www.youtube.com/watch?v=CqOfi41LfDw

[35] https://yarpiz.com/50/ypea102-particle-swarm-optimization